USGS
science for a changing world

Prepared in cooperation with National Park Service

Sample Descriptions and Geophysical Logs for Cored Well BP-3-USGS, Great Sand Dunes National Park, Alamosa County, Colorado

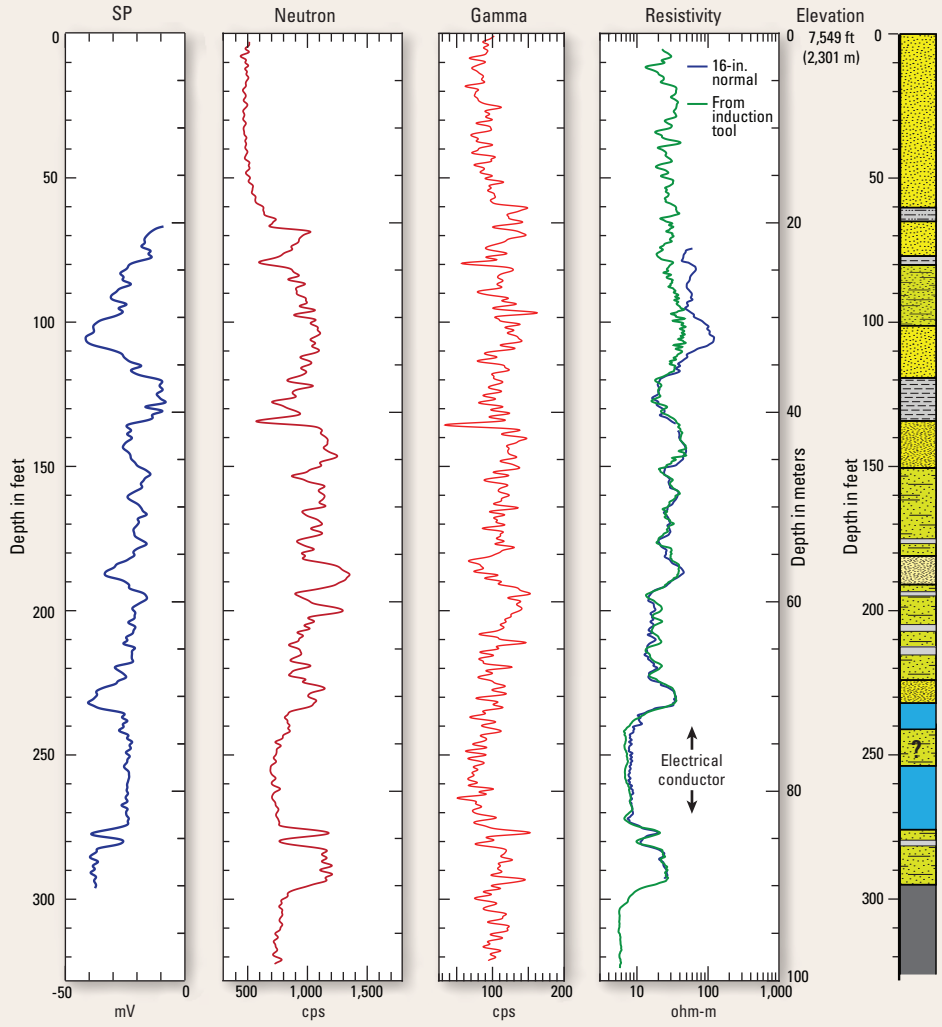

Data Series 918

U.S. Department of the Interior
U.S. Geological Survey

Cover. Selected generalized geophysical logs and generalized lithologic logs for BP-3-USGS.
Photographs from top to bottom:

At the end of a core run, the barrel is lifted out of the hole onto one of the several sawhorse setups.
Clay from the same sample as in A after almost 5 years of storage in a plastic bag.
Stream of water that was flowing out of the drill stem into the mud pool the morning of September 17, 2009.
Clay with blue tint at time of collection as a core catcher sample at 266 ft depth (core run 19). B, Clay with even-gray color at time of collection from ≈311 ft depth (core run 26).
Intact core after extrusion onto a split half of polyvinyl chloride pipe on a sawhorse apparatus.

Sample Descriptions and Geophysical Logs for Cored Well BP-3-USGS, Great Sand Dunes National Park, Alamosa County, Colorado

By V.J.S. Grauch, Gary L. Skipp, Jonathan V. Thomas, Joshua K. Davis, and Mary Ellen Benson

Prepared in cooperation with National Park Service

Data Series 918

U.S. Department of the Interior
U.S. Geological Survey

U.S. Department of the Interior
SALLY JEWELL, Secretary

U.S. Geological Survey
Suzette M. Kimball, Acting Director

U.S. Geological Survey, Reston, Virginia: 2015

Suggested citation:
Grauch, V.J.S., Skipp, G.L., Thomas, J.V., Davis, J.K., and Benson, M.E., 2015, Sample descriptions and geophysical logs for cored well BP-3-USGS, Great Sand Dunes National Park and Preserve, Alamosa County, Colorado: U.S. Geological Survey Data Series 918, 53 p., http://dx.doi.org/10.3133/ds918.

ISSN 2327-638X (online)

Contents

Figures

Tables

Appendix Tables

Download Files

Log files—data for borehole geophysical logs
http://pubs.usgs.gov/ds/0918/downloads/LogFiles/

Photographs of samples taken onsite
http://pubs.usgs.gov/ds/0918/downloads/PhotoFiles/

Conversion Factors

Inch/Pound to SI

Multiply	By	To obtain
	Length	
inch (in.)	2.54	centimeter (cm)
inch (in.)	25.4	millimeter (mm)
foot (ft)	0.3048	meter (m)
mile (mi)	1.60934	kilometer (km)
	Density	
grams per cubic centimeter (g/cm^3)	1,000.0	kilograms per cubic meter (kg/m^3)
	Velocity	
foot per second (ft/s)	0.3048	meter per second (m/s)
	Flow rate	
gallon per minute (gal/min)	0.06309	liter per second (L/s)
	Electrical resistivity	
ohm-meters (ohm-m)	0.001	kiloohm-meters (kohm-m)
	Electrical conductivity	
millimhos per meter (mmhos/m)	1,000.0	siemens per meter (S/m)
	Electrical potential	
millivolts (mV)	1,000.0	volts (V)

Supplemental Information

Electrical resistivity ρ in ohm-meters (ohm-m) can be converted to electrical conductivity σ in siemens per meter (S/m) as follows: $\sigma = 1/\rho$.

Datums

Vertical coordinate information is referenced to the North American Vertical Datum of 1988 (NAVD 88).

Horizontal coordinate information is referenced to the North American Datum of 1983 (NAD 83).

Elevation, as used in this report, refers to distance above the vertical datum.

Abbreviations Used in This Report

cps	counts per second
EM	electromagnetic
ka	kilo-annum (thousand years)
Ma	Mega-annum (million years)
NPS	National Park Service
PVC	polyvinyl chloride
TEM	time-domain electromagnetic
USGS	U.S. Geological Survey

Sample Descriptions and Geophysical Logs for Cored Well BP-3-USGS, Great Sand Dunes National Park, Alamosa County, Colorado

By V.J.S. Grauch,[1] Gary L. Skipp,[1] Jonathan V. Thomas,[1] Joshua K. Davis,[2] and Mary Ellen Benson[1]

Abstract

The BP-3-USGS well was drilled at the southwestern corner of Great Sand Dunes National Park in the San Luis Valley, south-central Colorado, 68 feet (ft, 20.7 meters [m]) southwest of the National Park Service's boundary-piezometer (BP) well 3. BP-3-USGS is located at latitude 37°43′18.06″N. and longitude 105°43′39.30″W., at an elevation of 7,549 ft (2,301 m). The well was drilled through poorly consolidated sediments to a depth of 326 ft (99.4 m) in September 2009. Water began flowing from the well after penetrating a clay-rich layer that was first intercepted at a depth of 119 ft (36.3 m). The base of this layer, at an elevation of 7,415 ft (2,260 m) above sea level, likely marks the top of a regional confined aquifer recognized throughout much of the San Luis Valley. Approximately 69 ft (21 m) of core was recovered (about 21 percent), almost exclusively from clay-rich zones. Coarser grained fractions were collected from mud extruded from the core barrel or captured from upwelling drilling fluids. Natural gamma-ray, full waveform sonic, density, neutron, resistivity, spontaneous potential, and induction logs were acquired. The well is now plugged and abandoned.

This report presents lithologic descriptions from the well samples and core, along with a compilation and basic data processing of the geophysical logs. The succession of sediments in the well can be generalized into three lithologic packages: (1) mostly sand from the surface to about 77 ft (23.5 m) depth; (2) interbedded sand, silt, and clay, decreasing in overall grain size downward, from 77 to 232 ft (23.5 to 70.7 m) depth; and (3) layers of massive clay alternating with layers of fine sand to silt from 232 to 326 ft (70.7 to 99.4 m), the total depth of the well. The topmost clay layers of the deepest package have a blue tint, prompting a correlation with the "blue clay" of the San Luis Valley that is commonly considered as the top of the confined aquifer. However, a confining clay was intercepted 113 ft (34.4 m) higher than the blue clay in BP-3-USGS.

Most of the geophysical logs have good correspondence to the lithologic variations in the well. Exceptions are the gamma-ray log, which is likely affected by naturally occurring radiation from abundant volcanic detritus, and one interval within the deepest lithologic package, which appears to be abnormally electrically conductive. Resistivity logs and variations in sand versus clay content within the well are consistent with electrical resistivity models derived from time-domain electromagnetic geophysical surveys for the area. In particular, the topmost blue clay corresponds to a strong electrical conductor that is prominent in the electromagnetic geophysical data throughout the park and vicinity.

BP-3-USGS was sited to test hypotheses developed from geophysical studies and to answer questions about the history and evolution of Pliocene and Pleistocene Lake Alamosa, which is represented by lacustrine deposits sampled by the well. The findings reported here represent a basis from which future studies can answer these questions and address other important scientific questions in the San Luis Valley regarding geologic history and climate change, groundwater hydrology, and geophysical interpretation.

Introduction

The U.S. Geological Survey (USGS) has been conducting geologic and geophysical studies for several years in the San Luis Valley, Colorado, under the auspices of the National Cooperative Geologic Mapping Program. The goals are to improve understanding of the present-day geologic framework in three dimensions and its geologic history. A combination of drill-hole information, geophysical methods, and geologic mapping provide the most comprehensive approach to determining the third dimension of geology that underlies the landscape.

One focus of the USGS studies has centered on the evolution and nature of deposits left behind by a large lake that occupied most of the San Luis Valley in the Pliocene and Pleistocene (Siebenthal, 1910). Recent geologic investigations conclude that this ancient Lake Alamosa formed about

[1]U.S. Geological Survey.

[2]University of Texas at Austin.

3 million years ago when lava erupted onto the valley floor and created a dam (Machette and others, 2013). The lake eventually breached the dam and drained out to form the throughgoing, modern Rio Grande drainage system several thousand years ago (Machette and others, 2007, 2013). However, the exact timing and nature of the lake's demise are still debated (Madole and others, 2013).

The deposits from the lake, known as the Alamosa Formation, include massive clay layers colloquially known as the "blue clay" that are penetrated by water wells throughout the San Luis Valley (Huntley, 1979a). The clays form barriers to groundwater flow, so they are important for understanding groundwater resources of the San Luis Valley, the primary water supply for its thriving agricultural community. Water resource managers in the valley use the depth and extent of the clays to define regulations for well pumping from an upper unconfined aquifer versus a lower confined aquifer. Knowledge of the thickness of, depths to, and lateral extents of these clays are also important for developing regional groundwater models, which are used to develop water resource management plans (for example, the Rio Grande Decision Support System, http://cdss.state.co.us/basins/Pages/RioGrande.aspx, accessed September 2014).

The National Park portion of Great Sand Dunes National Park and Preserve is located in east-central San Luis Valley, Colorado (fig. 1). The area overlies the eastern limit of the confining clay layers of the Alamosa Formation, but the depths to clay and limits of its extent are poorly known because of the extensive sand cover. To help address these unknowns and aid the National Park Service (NPS) in meeting their needs to better understand their groundwater resources, USGS geophysical efforts have focused on the National Park area. Several geophysical surveys were conducted over the park and vicinity, including time-domain electromagnetic (TEM) soundings and airborne surveys designed to image electrical resistivity as much as 984 ft (300 m) deep. As with electrical borehole logs, geophysicists use variations in electrical resistivity (or its inverse, electrical conductivity) in sand-clay environments to infer variations in sediment grain size and water quality with depth (Keys, 1990, 1997; Fitterman and Labson, 2005; Knight and Endres, 2005). Preliminary findings from the TEM soundings identified a strong electrical conductor that could be generally correlated with the presence of blue clay recorded in a few deep wells in the vicinity of the park (Fitterman and de Souza Filho, 2009; Fitterman and Grauch, 2010). A subsequent airborne TEM survey consistently detected this electrical conductor over a wider area of the park (Bedrosian and others, 2012; Grauch and others, 2013). Although correlations between the geophysical survey results and the lithologies in the wells appear good, the sparse and sometimes poorly documented well information does not provide a comprehensive test of the hypotheses.

A cored well, which collects whole samples rather than cuttings, provides a key to testing hypotheses developed from the geophysical studies and answers questions about the history and evolution of Lake Alamosa. Therefore, when the NPS began plans to drill 10 groundwater-monitoring wells along the western boundary of Great Sand Dunes National Park in 2009 (HRS Water Consultants, 2009; Harmon, 2010), the USGS proposed a supplemental cored well using the same drilling crew. A site was chosen adjacent to the NPS boundary-piezometer well BP-3, at the southwest corner of the park (fig. 1). The choice was guided by the results of TEM soundings collected at each of the 10 boundary-piezometer well sites before drilling began (D.V. Fitterman, USGS, unpub. report, 2009). The BP-3 site offered a reasonable, predicted depth of 235 ft (72 m) to the electrical conductor, inferred to be massive clay. This prediction turned out to be fairly accurate.

The BP-3-USGS well is located at latitude 37°43′18.06″N. and longitude 105°43′39.30″W., or 435,879E., 4,175,185N. (meters) using a Universal Transverse Mercator zone 13 map projection with North American Datum of 1983. The well was drilled through poorly consolidated sediments from a surface elevation of 7,549 ft (2,301 m) (NAVD 88 vertical datum) to a total depth of 326 ft (99.4 m) from September 14 through 17, 2009. It was sited 69 ft (21 m) southwest of the much shallower NPS boundary-piezometer well BP-3, with total depth of only 79 ft (24 m).

Water began flowing from the BP-3-USGS well once drilling reached a depth of 141 ft (43.0 m) after penetrating a clay-rich layer that was first intercepted at a depth of 119 ft (36.3 m), elevation 7,430 ft (2,265 m). Approximately 69 ft (21 m) of core was recovered (about 21 percent), almost exclusively from clay-rich zones. Coarser grained fractions were collected as viscous fluid extruded from inside the core barrel or captured from upwelling drilling fluids. Wireline geophysical logs acquired include natural gamma-ray, full waveform sonic, density, neutron, resistivity, spontaneous potential (SP), and induction logs. The well is now plugged and abandoned. Drilling and logging of BP-3-USGS was accomplished by the USGS Central Region drilling unit. Funding was provided by the National Cooperative Geologic Mapping Program. NPS, as well as HRS Water Consultants, Inc., who were contracted to oversee the 10 other wells, provided logistical support and technical advice.

Due to unanticipated limitations of personnel and resources after drilling was completed, systematic examination of the well samples and additional processing of geophysical logs did not begin until the end of 2013. This report presents the results of these efforts and includes information obtained from a 2012 study, which was limited to an examination of only core samples. We present basic lithologic descriptions of all the well samples, information on fossil occurrence, and data for geophysical logs for BP-3-USGS after basic data processing. A previous report details digital signal processing of the full waveform sonic log (Burke, 2011). All core and other types of samples from the well are archived at the USGS Core Research Center in Denver, Colo. (see http://geology.cr.usgs.gov/crc/).

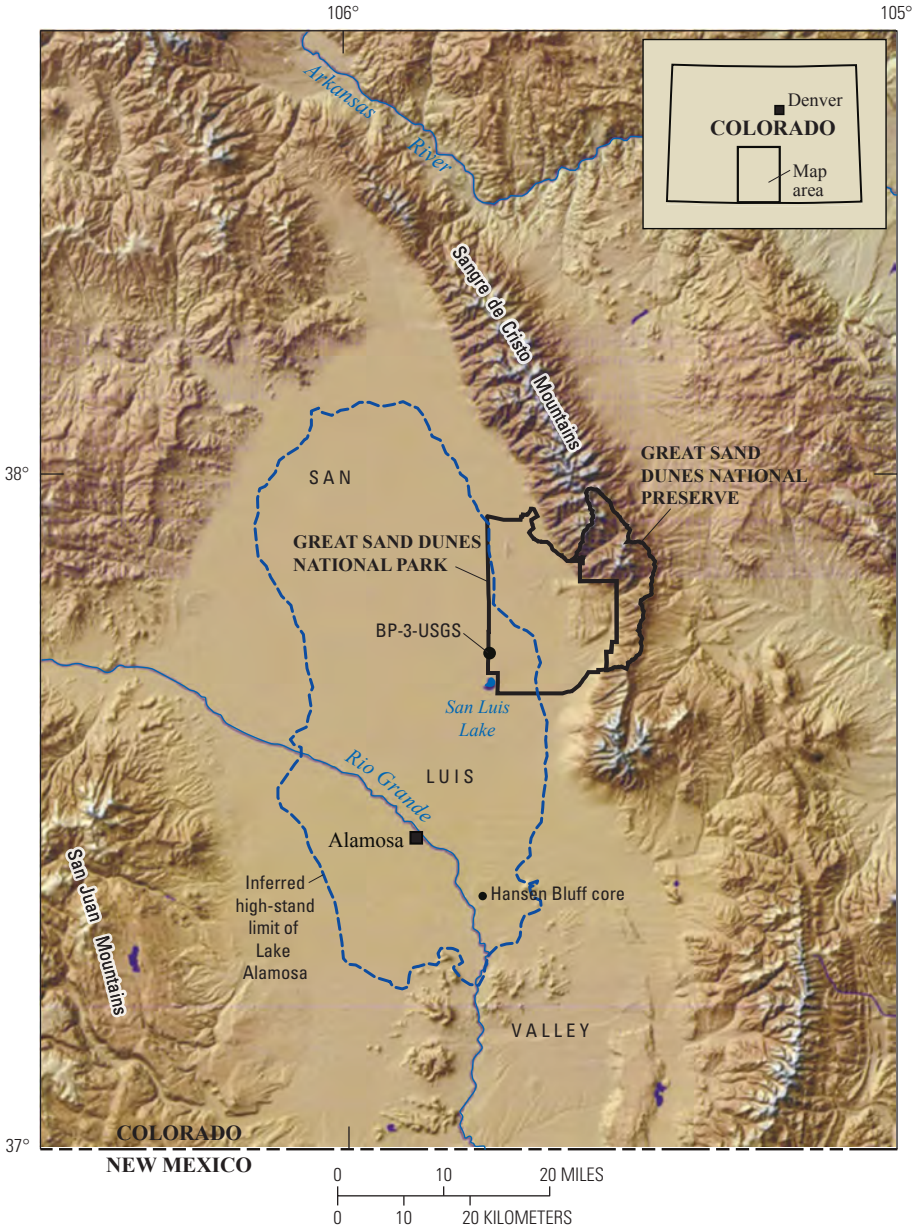

Figure 1. Location of BP-3-USGS well, the inferred limit of the last high stand of Pliocene and Pleistocene Lake Alamosa before its disappearance (from Machette and others, 2013), and the Hansen Bluff core site near Great Sand Dunes National Park and Preserve in Alamosa County of southern Colorado.

Regional Setting and Geophysical Studies

Great Sand Dunes National Park and Preserve is located at the eastern margin of the San Luis Valley in Colorado, nestled against an embayment in the Sangre de Cristo Mountains (fig. 1). The valley is underlain by thick deposits (up to thousands of meters) of poorly consolidated sediments that accumulated over the past 25–30 million years during basin subsidence that accompanied the formation of the Rio Grande rift. Rifting continues today at the Sangre de Cristo Mountains front along one of the most seismically active faults in Colorado (Kirkham and Rogers, 1981; Ruleman and Machette, 2007). Great Sand Dunes National Park and Preserve is located over the deepest part of the Rio Grande rift basin in the valley, encompasses a segment of the paleoseismically active range-front fault, and covers the inferred eastern limit of the hydrologically important clays that underlie most of the San Luis Valley.

The Alamosa Formation is associated with Lake Alamosa, the large lake that occupied most of the San Luis Valley during the Pliocene and Pleistocene (Siebenthal, 1910; Machette and others, 2013). The formation consists of fluvio-lacustrine sediments, including massive clay to interbedded clay and sand as much as hundreds of meters thick (Huntley, 1979b). The sediments accumulated within tectonically subsiding rift basins while the lake was expanding and contracting in response to climate changes (Brister and Gries, 1994; Machette and others, 2013). Although lacustrine clastic

deposits have been mapped at the surface, most of the evidence of the massive clay left behind by the lake is found in wells (Huntley, 1979a,b; Machette and others, 2007, 2013). The number and thickness of clay layers increase from west to east across the San Luis Valley (Huntley, 1979b). After Lake Alamosa disappeared, the valley was covered by fluvial and eolian deposits. The margins of the valley were also episodically inundated by alluvial-fan and glacial deposits (Colman and others, 1985; Madole and others, 2008; Madole and others, 2013).

Multidisciplinary investigations of measured sections of the Alamosa Formation and a core hole collected near Hansen Bluff, 24 mi (38 km) to the south of the BP-3-USGS (fig. 1), provide detailed information about the lithology and depositional environment over time (Rogers and others, 1985, 1992). The core and surface samples comprise a sediment and fossil record from 2.67 to 0.67 million years ago (Ma [Megaannum]), as determined from paleomagnetic measurements on the samples and correlation of several ash layers to dated eruptions in the western United States. However, this section may not include the uppermost part of the Alamosa Formation, which should have persisted until at least 0.44 Ma (Machette and others, 2013). Several oil and gas wildcat wells also drilled through the Alamosa Formation, encountering thick clays, claystones, and fossil debris (Huntley, 1979b; Brister and Gries, 1994). Brister and Gries (1994) noted the presence of widely distributed, poorly cemented sandstone horizons near the top of the Alamosa Formation. They considered these horizons to mark the beginning of the demise of the lake.

Groundwater underlying San Luis Valley and Great Sand Dunes National Park primarily resides in two principal aquifers: a shallow unconfined aquifer and a deeper confined aquifer (Emery and others, 1973; Huntley 1979a; Hearne and Dewey, 1988). The shallowest impermeable clay layer within the Alamosa Formation (the blue clay) forms the separation between the two aquifers locally. The upper confining clay layer is generally found at depths of 40–100 ft (12.2–30.5 m) throughout the central part of the San Luis Valley, with depths >100 ft (30.5 m) toward the eastern side (Emery and others, 1973).

In the vicinity of the park, the unconfined aquifer is mainly composed of an eolian sand sheet overlying medium- to coarse-grained piedmont alluvium, which in turn overlies clay, silt, and fine-grained sand of the upper part of the Alamosa Formation (HRS Water Consultants, 1999; Madole and others, 2013). The permeability of the unconfined aquifer can be high but is widely variable (Huntley, 1979a). The unconfined aquifer in the vicinity of the park is primarily recharged from surface flow at the Sangre de Cristo Mountains front but mixes with precipitated water as it flows under the dune field (Rupert and Plummer, 2004). Some of the water discharges at local creeks; the rest flows southwestward and discharges in closed-basin lakes, such as San Luis Lake (fig. 1).

The deeper confined aquifer is composed of the lacustrine deposits of interbedded clay, sand, and gravel within the Alamosa Formation. The interbedded layers are difficult to correlate across the basin and have heterogeneous hydraulic properties (Hearne and Dewey, 1988). The extent of the confined aquifer is commonly mapped using the locations of artesian water wells (for example, Huntley, 1979a; Machette and others, 2007, 2013), although some wells completed in the confined aquifer are nonflowing (Brendle, 2002). Recharge to the confined aquifer occurs at the outer limits of the confining clays near the edges of the valley and flows into the discharge area near San Luis Lake (fig. 1) (Emery and others, 1973; Huntley, 1979a; Rupert and Plummer, 2004). Rupert and Plummer (2004) observed that the major ion chemistry of water from the confined aquifer in wells 7 mi (11 km) to the northeast of BP-3-USGS is distinct from that of the unconfined aquifer. They also determined that the confined water in one of these wells had resided in the basin for about 30,000 years. Data are lacking to determine whether the unconfined and confined aquifers are regionally connected (Huntley, 1979a; Rupert and Plummer, 2004).

Preliminary results from ground-based TEM geophysical methods (Fitterman and de Souza Filho, 2009; Fitterman and Grauch, 2010; Grauch and others, 2010) showed a highly resistive thin layer near the surface, a strong signal from an electrical conductor at depths of 150–330 ft (50–100 m), and a transitional layer of low electrical resistivity in between. The electrical conductor was interpreted as a regionally persistent, thick clay that correlates with the blue clay in the few existing deep wells in the area. The top resistive layer was interpreted as sand cover. The transitional layer was interpreted as fine-grained sediment, a combination of sand and clay, or both. Subsequent airborne TEM surveys confirmed these general observations, providing greater detail on the variations in depth and thickness of the three interpreted geophysical layers across a broad area of the park and vicinity (Bedrosian and others, 2012).

Drilling Operations

The drilling and geophysical logging were conducted by the USGS Central Region drilling unit located in Denver, Colorado, who were already on contract to NPS for the 10 wells they were drilling along the boundary of the park. Drilling was initiated on September 14, 2009, using a mud-rotary method for the first 60 ft (18.3 m) and coring methods thereafter. After coring from 60 to 80 ft (18.3 to 24.4 m) depth, 6-inch (in.) schedule 40 polyvinyl chloride (PVC) casing was set to a depth of 67 ft (20.4 m). Core sampling was attempted after every 10-ft (3.0-m)-depth interval, but the intervals varied from 2 ft (0.6 m) to 18 ft (5.5 m) to accommodate variations in sample recovery that depended on the quantity and distribution of clay. To acquire core samples, the 10-ft (3-m)-long core barrel was pulled from the well (fig. 2*A*). Rubber teeth within a metal fitting screwed to the bottom of the barrel, called a core catcher, are designed to let core travel up into the barrel but not fall out of it. After the core catcher and any sediment

Figure 2. Photographs of drilling operations. *A,* At the end of a core run, the barrel is lifted out of the hole onto one of the several sawhorse setups. *B,* Once placed, the core catcher is unscrewed from the bottom of the barrel and any sediment removed. *C,* The barrel is moved to a different sawhorse apparatus and the core extruded by a plunger inserted into the top. Pictured, left to right, are Steve Grant, Mike Williams, and Derek Gongaware, U.S. Geological Survey (USGS) drilling crew. *D,* The core and fluids are extruded onto a lengthwise split of polyvinyl chloride (PVC) pipe for sampling. *E,* Stream of water that was flowing out of the drill stem into the mud pool the morning of September 17, 2009. *F,* Setting up for borehole logging. The tools are stored in the PVC tubes lined up along the truck bed. The reel for the wire is partially visible at the top right of the photo. Pictured, left to right, Barbara Corland and Steve Grant, USGS. Photographs by V.J.S. Grauch (*A*–*E*) and Harland Goldstein (*F*).

trapped inside were removed from the end of the barrel, the remaining material was extruded from the barrel onto a lengthwise-split of PVC pipe that was lying on a saddle-horse apparatus (figs. 2*B*–2*D*).

Early on, it appeared that sands were flowing out of the core barrel and into the drilling mud, leaving very little material inside the barrel for sampling. Thus, the decision was made to pull the core barrel only for those 10-ft intervals where significant clay was encountered. Short intervals (<1 ft) of clay were sometimes all that was recovered as core. Below 261 ft (80 m) depth, the increased proportion of clay allowed for better core recovery and core runs (when the core barrel was pulled and samples were recovered) occurred at 2- to 7-ft (0.6 to 2.1-m)-depth intervals.

Bentonite mud was used during drilling below 90 ft (27.4 m) to keep the hole open after attempts to use water mixed with polymer in the interval 80 to 90 ft (24.4 to 27.4 m) proved unsuccessful. Groundwater began flowing out of the well at about 0.25 gallons per minute (gal/min) (0.016 liters per second [L/s]) once drilling reached 141 ft (43 m) depth. The flow rate had increased to 10–20 gal/min (0.631–1.26 L/s) by the time the drill stem was pulled for the night from 276 ft (84 m) depth on September 16. During the night, the artesian flow flushed out the drilling mud (fig. 2*E*), and the sides of much of the hole collapsed. The hole had to be reopened before coring could resume the next morning.

Coring was completed on September 17 at a depth of 326 ft (99.4 m) when the drilling budget was expended. The well was then logged using six different borehole tools (fig. 2*F*). The next day, the hole was plugged with cement and surface casing removed. The site was cleaned up and abandoned.

Procedures for Lithologic Descriptions

Lithologic descriptions of the well samples are included in appendix 1. The quality and accuracy of these descriptions are dependent on the sampling procedures, effects of subsequent storage and handling, laboratory methods employed, and strategies for positioning the samples relative to well depth. Some of these procedures proved challenging for BP-3-USGS; they are described in the following sections to provide context for the lithologic logging that was undertaken.

Sampling Procedures

Types of samples fall into one of two general categories depending on where the material was collected: core barrel samples or mud stream samples. Collection of material extruded from the core barrel was relatively straightforward. Other sampling strategies were required to collect sediment that moved out of the core barrel into the mud stream. Table 1 summarizes the types of samples and what they represent, with illustrative photos shown in figures 3 and 4. More detail is included in the following sections.

Mud Stream Samples

For the first 60 ft (18 m) of rotary drilling, sieves were placed in the mud pool next to the drill rig. Material was removed from a sieve at specified depth intervals and collected in plastic bags. The mud stream also flowed through a shale shaker, or hopper, which separated the sediment into coarse and fine fractions. Samples from the hopper were only collected occasionally at the shallower depths and put in plastic bags.

After core runs provided little material from 70 to 101 ft (21.3 to 30.8 m) depth, the drillers concluded that small amounts of clay were clogging the core catcher and forcing coarser grained sediment to come up with the drilling fluid rather than enter the barrel. As a result, samples from the mud stream received greater attention, and strategies were developed to capture sediment from the stream. Some experimentation was required, and the strategy evolved as drilling proceeded.

From 101 ft (30.8 m) to 119 ft (36.3 m), samples sieved from the mud stream were collected every few feet because drilling speed indicated mostly sand. When drilling speed slowed significantly through tighter material (presumably clay) from 119 ft (36.3 m) to 131 ft (39.9 m), the core barrel was pulled several times and sieve samples were not collected. Below 131 ft (39.9 m) depth, a new sampling strategy was employed to try to capture greater amounts of fine-grained material. In this strategy, mud flowing out of the casing during a 10-ft (3.0-m) drilling interval was collected periodically in a bucket. At the end of the interval, water was added and the bucket allowed to sit. After a time, the fluids were decanted and the remaining sediment collected in a plastic bag. Thus, bucket samples represent an amalgamation of sediment over an interval. With greater clay content in the lower depths of the well, very little material was obtained from bucket samples, especially in comparison to the volume recovered as core. Combined with observations that the lithologies of these later bucket samples were all very similar, we conclude that these bucket samples mostly represent sediment that was circulated by the drilling fluid from shallower parts of the well.

Core Barrel Samples

Material extruded from the core barrel included intact core or core pieces, viscous fluid (sediment slurry or water with suspended sediment or mud), and clay-rich sediments caught in the core catcher at the bottom of the barrel. Commonly, clay core became stuck in the barrel requiring extrusion using a power air hose. Two times the extrusion proved explosive and core ended up on the ground. One time, clay was stuck in the barrel and ended up attached to the subsequent core run. These incidents are noted in the lithologic descriptions (appendix 1).

The core catcher and the sediment within it were removed before material was extruded from the barrel. Sediment was removed from the core catcher with a scoop and placed in a

plastic bag, which was labeled with the core-run number and depth interval.

Intact core was extruded from the core barrel into a 10-ft (3.0-m)-long split of PVC pipe. It was measured, photographed, then transferred to another lengthwise split of PVC pipe that was 5 ft (1.5 m) long or shorter to match the length of the core. The 5-ft (1.5-m) maximum was chosen to facilitate core storage and handling. Most of the core was washed before it was wrapped in plastic, and the top split of the shorter PVC pipe placed on top. Any extra space within the pipe at the ends of the core was filled with floral foam before the two PVC halves were secured together with tape. The PVC and plastic wrap were labeled using the core-run number, depth interval, and an arrow indicating which end of the core is up (shallowest).

In a few cases (noted in appendix 1), intact core was divided into pieces. The reasons include (1) forcible extrusion ended with some of the core on the ground, so the original orientation was uncertain; (2) part of the core was deformed, so it was cut off and bagged; and (3) the core exceeded the 5-ft length of the PVC pipe used for storage, so that the core was divided.

Where viscous fluid was extruded instead of consolidated sediment, samples were collected using a scoop or by pouring the fluid through a sieve into a plastic bag (table 1; noted in appendix 1). The bags were labeled with the core-run number and depth interval.

Table 1. Explanation of and procedures for different sample types.

[PVC, polyvinyl chloride]

Sample type	Explanation and procedures	Illustrative figure
	Mud stream samples	
Sieved cuttings	Mud streaming out of the well and collecting in a sieve with medium-sized (1/16 inch) mesh. The sieve was pulled from the mud pool and sampled when drilling reached a specified depth. These types of samples were only collected for the top 60 ft (18.3 m) of depth, before coring commenced.	Figure 3*A*
Sieve sample	Mud streaming out of the well after passing through a sieve with medium-sized (1/16 inch) mesh. Samples collected when drilling reached a specified depth. These types of samples were collected only after coring had commenced.	Figure 3*B*
Hopper sample (coarse and fine fractions)	Samples collected from the mud stream after it was separated into coarse and fine fractions by a shale shaker (hopper).	
Bucket sample	Sediment collected as follows: Samples of mud flowing out of the well were periodically amassed into a bucket over a specified depth interval. After adding water, the bucket was left sitting in order for sediment to naturally separate from the fluid. The fluid was then decanted from the bucket and the remaining sediment collected.	Figures 3*C*, 3*D*
Hand sample	Hand selected specimens collected from a sieve sample or from the hopper.	
	Core barrel samples	
Core	Intact core or core segments that remained contiguous with one another in their original orientation as they were extruded into the lengthwise split of PVC pipe.	Figure 4*A*
Viscous fluid sample, scooped	Sample of water with suspended sediment or mud that flowed from the core barrel. High-viscosity samples were scooped directly into a plastic bag.	Figure 4*B*
Viscous fluid sample, sieved	Sample of water with suspended sediment or mud that flowed from the core barrel. Low-viscosity fluids were sieved before collecting in a plastic bag.	Figure 4*C*
Core catcher sample	Sample of sediment caught inside the core catcher, a metal fitting at the bottom of the core barrel. Only clay-rich sediments were trapped by the core catcher, so thin clay beds within sandy intervals were sampled preferentially.	Figure 4*D*
Core piece	A short piece of intact core placed in a bag rather than in PVC pipe.	

Figure 3. Photographs of various sampling procedures for mud stream samples. *A,* A cuttings sample is sieved and collected from the pool of mud next to the drill stem during the first 60 feet of rotary drilling. *B,* A sieve sample is collected from the mud stream while coring. The sieve, attached to a long handle, collects mud that is streaming up the sides of the core barrel and out of the hole. *C,* Mud streaming from the hole is collected periodically in a small bucket and emptied into a large bucket during the collection of a bucket sample. Pictured, left to right, Steve Grant and Jeff Eman, U.S. Geological Survey (USGS). *D,* At the end of the drilling interval, fluid from the large bucket is decanted and the remaining sediment stored as the bucket sample. Pictured, left to right, Jeff Eman and Harland Goldstein, USGS. Photographs by V.J.S. Grauch.

Figure 4. Photographs of various sampling procedures for core barrel samples. *A,* Intact core after extrusion onto a split half of polyvinyl chloride (PVC) pipe on a sawhorse apparatus. *B,* Viscous fluid collected with a shovel from poorly consolidated core that was extruded along with intact core (not shown). *C,* Viscous fluid poured through a sieve from the core barrel and collected as a sieved sample. *D,* Example of a core catcher sample before it was bagged. After detaching the core catcher at the bottom of the core barrel, sediment is inside the fixture and extending outside. Most other core catcher samples did not extend this far outside the fixture. Photographs by V.J.S. Grauch.

Effects of Storage and Handling

During the more than 4 years that samples were stored before examination, most of them dried out. Much of the clay making up the core samples contracted and broke into smaller pieces. Thus, the core was never split, fearing that such attempts would further disintegrate the samples. The bagged samples fared better; some of these retained a little of the original fluid that had been captured along with the sediment. Additional problems for the clay-rich samples were changes in color and biologic growth observed since acquisition, suggesting that chemical reactions had taken place. As a result, accurate color descriptions and chemical sampling were not attempted.

The desiccation and disaggregation of the clay-rich core samples affected measurements of core length between collection and examination. Shrinkage was most notable for the core samples containing the most clay, at depths below 261 ft (79.6 m). On the other hand, disaggregation of the desiccated core also resulted in expansion of total length because the pieces tended to separate and leave cracks between them. This problem is exacerbated by repeated handling of the core. Table 2 lists measured core lengths at original acquisition compared to two subsequent episodes of examination showing where core length has varied.

Photographs that capture how samples appeared at the drill site may be downloaded from the Photos folder, which also includes an index file describing the contents of the photographs. These photos are the best record of the conditions of the samples at the time they were collected, especially regarding color and sedimentary structures. Figure 5 shows an example of a clay-rich piece of core as it looked at the time of its collection compared to its appearance after more than 4 years of storage. Note the change in color and obscuring of oval blotches of different color that may be part of an important biogenic or sedimentary feature. Figure 6 demonstrates how the subtle color differences between samples from blue versus gray clay are obvious right after collection, but not so after they dried out.

Table 2. Core lengths recovered onsite in 2009 and changes in measured lengths in years 2012 and 2013.

[cm, centimeter; --, no data; %, percent]

Core run*	Drilling depth interval, in feet	Core length recovered in 2009, in inches (cm)	2012 measured length, in inches (cm)	2013 measured length, in inches (cm)	2012 change from 2009	2013 change from 2009
9	125–128	12.0 (30.5)	--	12.0 (30.5)	--	0.0 %
11	131–141	7.5 (19.1)	7.9 (20.0)	10.0 (25.4)	+5.0 %	+33 %
13	171–191	47.0 (119.4)	47.2 (120.0)	48.0 (121.9)	+0.5 %	+2.1 %
14	191–201	38.0 (96.5)	35.4 (90.0)	37.0 (94.0)	–6.8 %	–2.6 %
15	210–211	20.0 (50.8)	20.1 (51.0)	20.0 (50.8)	+0.4 %	0.0 %
16	211–221	26. 0 (66.0)	24.8 (63.0)	26.0 (66.0)	–4.6 %	0.0 %
17 (top)	231–241	57.5 (146.1)	55.9 (142.0)	57.5 (146.1)	–2.8 %	0.0 %
17 (bottom)	231–241	29.8 (75.6)	28.3 (72.0)	29.4 (74.7)	–4.7 %	–1.2 %
18 (top)	251–261	57.5 (146.1)	51.6 (131.0)	57.5 (146.1)	–10 %	0.0 %
18 (bottom)	251–261	17.0 (43.2)	13.8 (35.0)	17.0 (43.2)	–19 %	0.0 %
19	261–266	54.0 (137.2)	45.7 (116.0)	48.0 (121.9)	–15 %	–11 %
20	266–271	45.5 (115.6)	39.4 (100.0)	42.0 (106.7)	–13 %	–7.7 %
21	271–276	44.0 (111.8)	35.4 (90.0)	38.0 (96.5)	–20 %	–14 %
22	276–291	11.0 (27.9)	9.1 (23.0)	10.0 (25.4)	–18 %	–9.1 %
23	291–301	59.0 (149.9)	57.9 (147.0)	60.0 (152.4)	–1.9 %	+1.7 %
24	301–306	60.0 (152.4)	56.3 (143.0)	60.0 (152.4)	–6.2 %	0.0 %
25	306–311	24.0 (61.0)	22.8 (58.0)	23.0 (58.4)	–4.9 %	–4.2 %
26	311–316	57.0 (144.8)	54.3 (138.0)	54.0 (137.2)	–4.7 %	–5.3 %
27	316–321	60.0 (152.4)	53.2 (135.0)	54.0 (137.2)	–11 %	–10 %
28	321–326	55.0 (139.7)	49.6 (126.0)	52.0 (132.1)	–9.8 %	–5.5 %

*Core was not recovered from all core runs. Cores recovered from runs 17 and 18 were divided into top and bottom pieces on site and stored separately.

Figure 5. Photographs of a selected core at time of collection compared to more than 4 years later. *A,* Washed core piece from the bottom of core run 25 (depths 306–311 ft) on September 17, 2009. Note the dark oval splotch that may be a sedimentary structure or trace fossil. *B,* The same core piece as it looked on February 5, 2014, after it had been wrapped in plastic and stored inside a polyvinyl chloride (PVC) pipe. Note the color change, breakage, and difficulty seeing the oval splotch. Photographs by V.J.S. Grauch (*A*) and Gary L. Skipp (*B*).

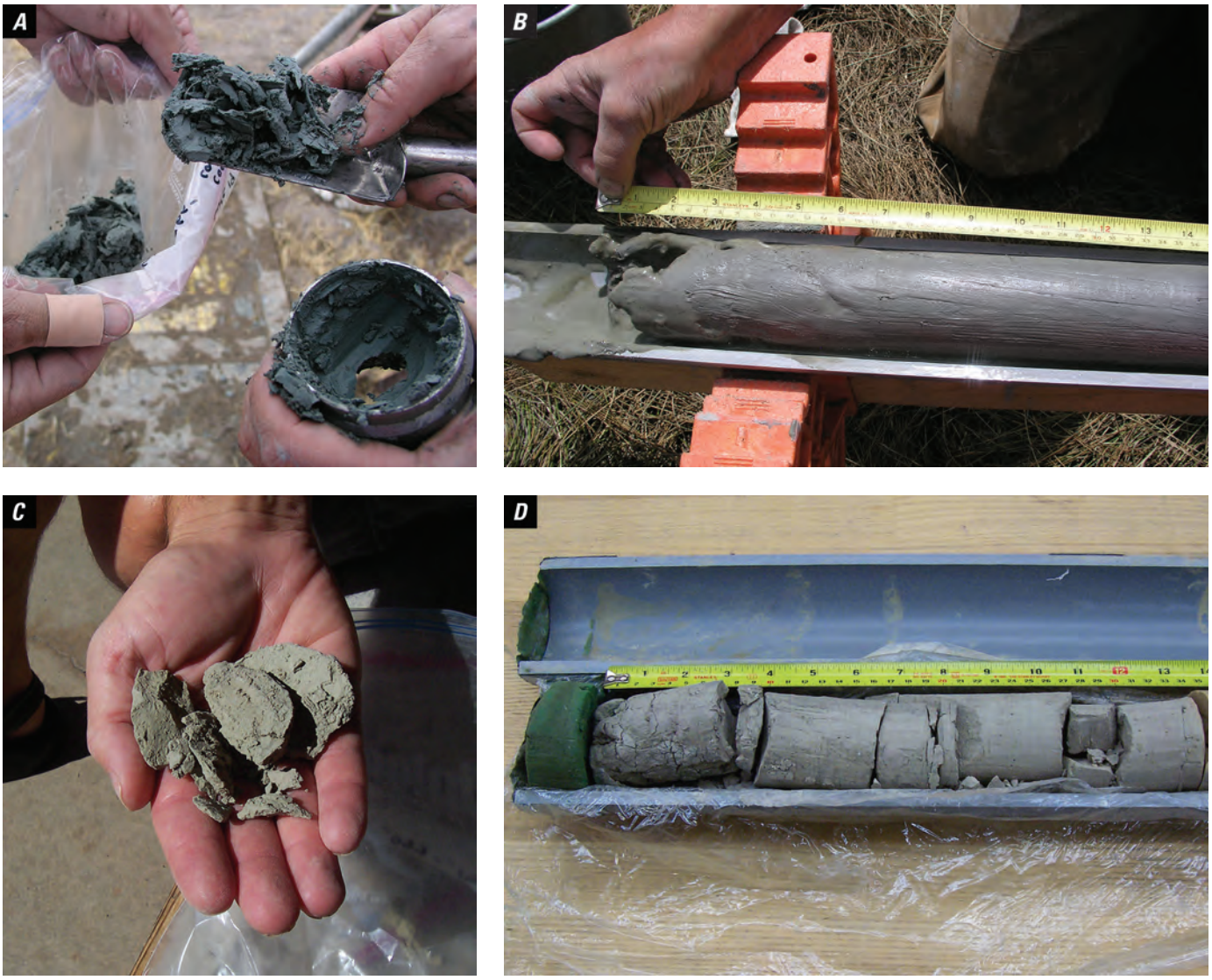

Figure 6. Photographs of two clay samples of differing color at time of collection in September 2009 compared to almost 5 years later in August 2014. *A,* Clay with blue tint at time of collection as a core catcher sample at 266 ft depth (core run 19). *B,* Clay with even-gray color at time of collection from ≈311 ft depth (core run 26). *C,* Clay from the same sample as in *A* after almost 5 years of storage in a plastic bag. Note the color change. *D,* Clay from the same core sample as in *B* after almost 5 years of storage wrapped in plastic in a polyvinyl chloride (PVC) pipe. Note the extensive disaggregation and the color change for a small piece of the core on the right-hand side of the photo. Photographs by V.J.S. Grauch (*A* and *B*) and Gary L. Skipp (*C* and *D*).

Laboratory Methods

All samples from the well were examined and described regarding grain sizes, types, and shapes; sorting, layering, and sedimentary structures; calcium carbonate content; occurrence of fossils or other biogenic material; evidence of biologic activity such as trace fossils or bioturbation; and presence of volcanic ash (appendix 1). Some samples were examined for mineralogy using X-ray diffraction analysis. Difficulties in sample recovery and the effects caused by the long period of sample storage affect how well these descriptions actually represent the lithology at depth. Specific depths that were sampled are uncertain for core samples that are shorter in length than the drilling depth interval.

Bagged samples from the drilling and coring were first identified as to type of sample (table 1). Cores were first wetted with a spray bottle then scraped to a depth of several millimeters on a portion of the core over the entire length. Scraping was done to remove core barrel smear contamination. Wetting was done for visual enhancement of any structures present (bedding, laminations, faulting, bioturbation, contacts, grain size changes, and so forth). Because some of the core had fragmented, a representative piece within broken intervals was chosen for wetting and scraping.

Both bagged and core samples were then examined under a binocular microscope to observe grain size and shape, sorting, grain color, and some mineralogy. The relative quantity of calcium carbonate (calcareous degree) was estimated from the intensity of effervescence after application of a 10-percent solution of hydrochloric acid (HCl). Core samples were tested every few inches. Samples suspected to contain fossils or unusual mineral assemblages were viewed under the binocular microscope. Some such samples were tested for magnetic grains using a magnet. Several samples were chosen for X-ray diffraction analysis to determine mineralogy. A subset of these samples were mounted (smear slide) for petrographic examination.

Occurrences of animal remains and evidence of biologic activity were noted during the systematic examination of bagged and core samples in 2013 by G.L. Skipp and by M.E. Benson and J.K. Davis while studying core samples in 2012. Most fossil specimens were categorized as bivalves, gastropods, ostracods, or unidentified shells. A few samples were examined by M.E. Benson for the potential presence of diatoms. Where diatoms were found, they were preliminarily identified. Bones and teeth were distinguished, where possible, but no effort was made to identify the animal type, as remains were not intact. Other evidence of animal or plant life included fine organic debris, woody plant parts, or bioturbation, none of which was researched in detail. Appendix 2 provides descriptions of the fossils or other evidence of life and the depth intervals where they were observed. Because core length measurements differed between the 2012 and 2013 studies, the locations of the occurrences within the core samples are listed separately and should be considered approximate for future work.

Samples taken for X-ray diffraction analysis were ground to <200 mesh size (≈10 micrometer [μm]) and packed into a cavity mount. Analysis was performed on a Philips R150 goniometer with a XRG3100 generator using a 2°-theta scan range of 6–65. Resulting X-ray diffraction patterns were evaluated for characteristic patterns of common minerals. The resulting bulk mineralogy for each sample is listed in appendix 3.

Sample Descriptions Versus Well Depths

Findings from the sample descriptions detailed in appendix 1 are depicted graphically versus well depth in figure 7, divided in two columns by sample type. Assigning the findings to specific depths within the well is not straightforward due to uncertainties caused by poor core recovery and difficulties in sampling sands. The uncertainties, and thus how depths were estimated, are different for mud stream versus core barrel samples. For mud stream samples collected over specific depth intervals, uncertainties arose as to whether they accurately represent the sediment in the well over that interval. For core samples that were shorter than their associated drilling interval, uncertainties arose regarding their positions within that interval.

Mud stream samples collected during the first 60 ft of rotary drilling (sieved cuttings and hopper samples) were obtained as cuttings of all sediment and are considered to adequately represent the intervals they sampled. Below this depth, sieve and bucket samples were also collected for specified depth intervals, but the sediment may not adequately represent the sediment within that depth interval because of possibilities of mixing with sediment from uphole depths. On the other hand, the volume retrieved in bucket samples significantly decreased as more clay was recovered as core. This correlation, along with very similar lithology noted for these minimal-volume samples, suggests that the quantity of contaminating material was limited. In any case, bucket samples with minimal volume are not reliable samples, because they may not be representative of the depth interval sampled, and are noted with question marks on figure 7.

Depth placement of most core samples was evaluated using matches of the lithology of the sample to the description of sediment encountered in the interval onsite and supporting evidence from the geophysical logs. Some matches relied primarily on the geophysical logs. Depth intervals of core could also be estimated relative to the underlying core catcher sample. Depths were generally easier to estimate for core catcher samples because they commonly represented the last clay recognized by drilling speed before the driller pulled the core barrel. In all but one case, core that was extruded from the barrel in pieces could be considered contiguous. The one exception is core run 13 (depth interval 171–191 ft), where core was extruded as many pieces (4-ft total length) along with viscous fluid (appendix 1 and fig. 7). If the many pieces were considered contiguous, the clay and cemented sand layers observed did not match in depth compared with relative low- versus high-resistivity values in the geophysical logs. The matches were improved if a gap in core recovery was inferred.

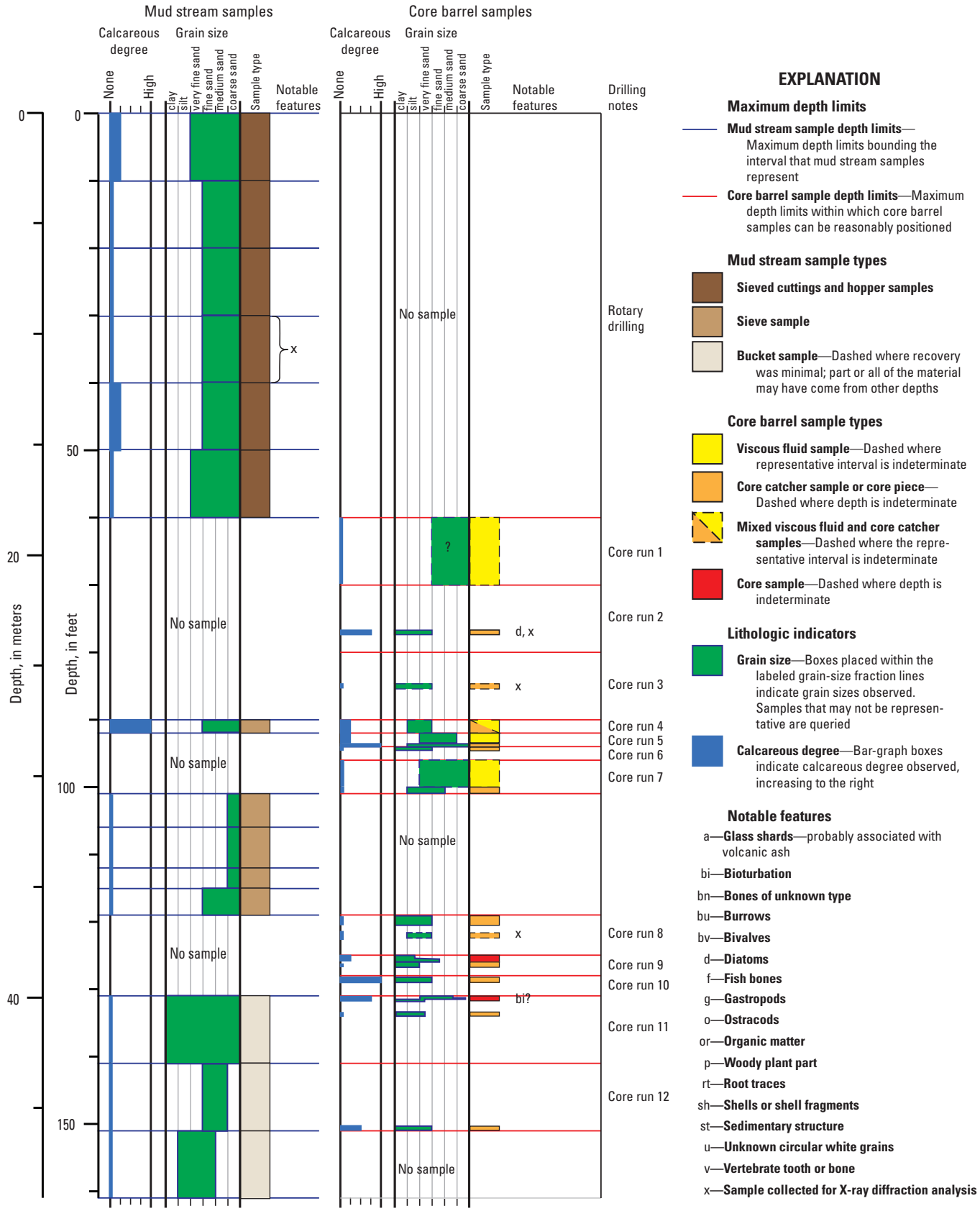

Figure 7. Graphical summary of lithologic descriptions and other observations versus inferred well depth. More detail and explanatory material can be found in appendixes 1 and 2. Because knowing the sample type is important for understanding the significance of the observations and for inferring depth ranges of the samples, two columns divided by sample type are shown side by side. The positions of the codes for notable features only approximately depict where they are positioned relative to core samples.

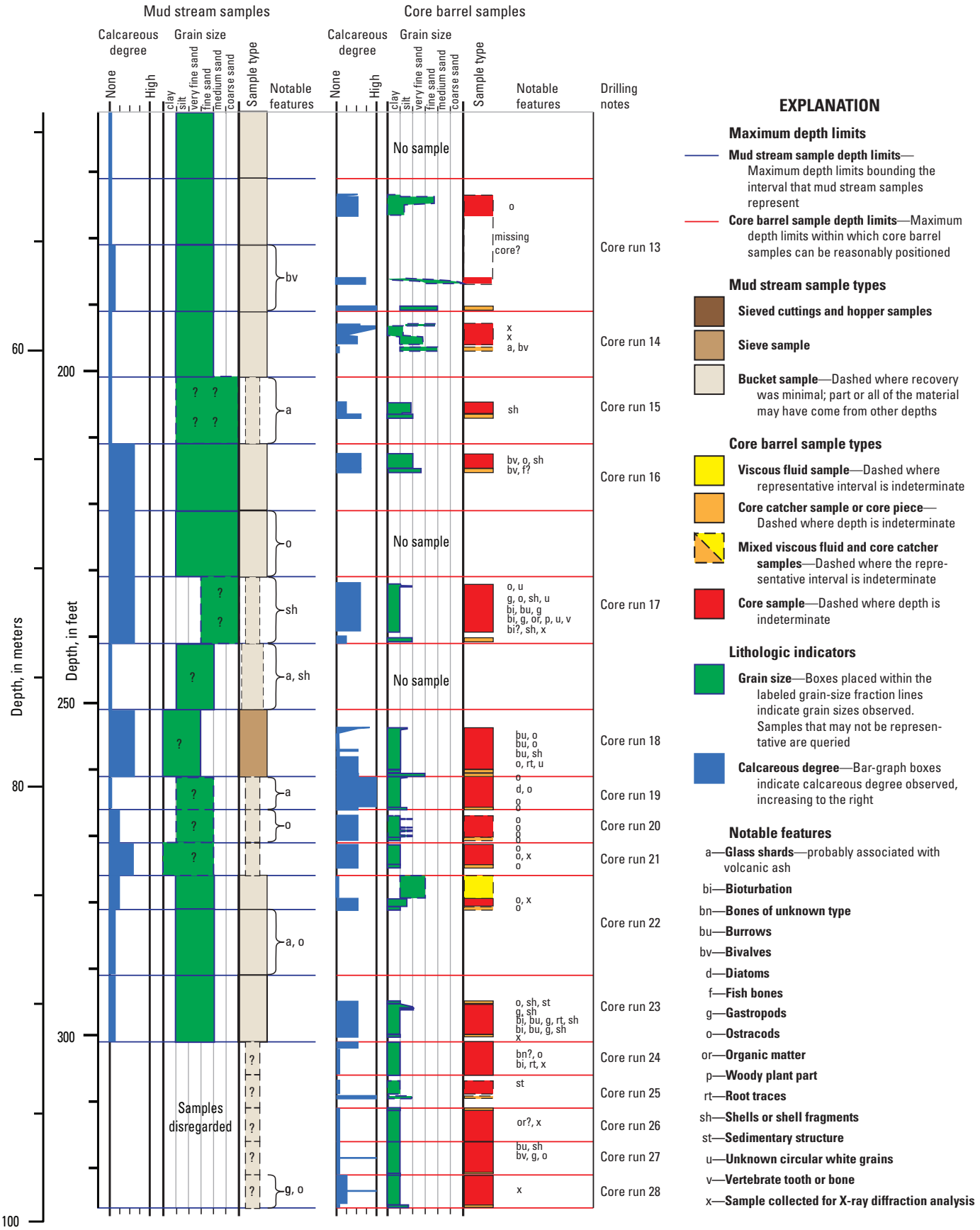

Figure 7. Graphical summary of lithologic descriptions and other observations versus inferred well depth. More detail and explanatory material can be found in appendixes 1 and 2. Because knowing the sample type is important for understanding the significance of the observations and for inferring depth ranges of the samples, two columns divided by sample type are shown side by side. The positions of the codes for notable features only approximately depict where they are positioned relative to core samples.—Continued

Most depth estimates have fair confidence. Those with uncertainties are indicated by dashed outlines on figure 7. In all cases, maximum errors on the position of the core samples are defined by the upper and lower limits of the drilling depth interval (red lines on fig. 7). Uncertainties for three core runs are particularly large, for which the maximum errors apply (runs 3, 13, and 14; fig. 7).

The depths that viscous fluid samples represent are all uncertain, so all outlines for these sample types are dashed on figure 7. Although the fluid must have sampled the depth interval indicated, it is likely that the entire volume of that interval is not adequately represented. In some cases, the relation of the viscous fluid to more solid portions of the core barrel sample was obvious after extrusion from the barrel, so the depth uncertainties are somewhat less.

Geophysical Logs

Six wireline geophysical tools were used to obtain logs of natural gamma-ray, electrical resistivity and conductivity, spontaneous potential, full waveform sonic, density, and neutron data and several other borehole parameters. These logs were chosen to augment lithologic interpretations of the well and to investigate physical properties of the subsurface that can be correlated to surface geophysical measurements and to other wells in the region.

Logs Acquired

Table 3 lists the tools and associated logs in the order they were obtained. Each tool was lowered as close as possible to the bottom of the hole, then data were collected at 0.1-ft (3-centimeter [cm]) intervals as the tool was raised.

Table 4 presents the simplified responses for the logs and their corresponding inferred physical parameters, modified from Keys (1990, 1997). Also noted in table 4 are the types of responses important for interpreting lithology from the logs measured in BP-3-USGS. Readers are referred to Keys (1990, 1997) for additional information on interpreting the logs for other parameters, such as water quality and porosity.

Data Processing

Measurements originally recorded at specific times by each geophysical tool as it was raised by winding up its attached wire were converted to depth measurements using the number of rotations of the wire reel and industry-supplied coefficient values. (The reel is partially shown in fig. 2*F*). The depth measurements were then interpolated as a sequence of evenly spaced data points, generally using a depth spacing of 0.1 ft (≈3 cm). The resulting sequences of data points, representing measurements every 0.1 ft (≈3 cm) down the hole, can then be manipulated using standard borehole and geophysical processing techniques. After basic processing by the logging

Table 3. Geophysical tools and associated data logs acquired for BP-3-USGS, listed in the order they were acquired.

Tool type	Tool model*	Logs acquired	Comments on data collected
Gamma-caliper	Century Geophysical 9074	Three-arm caliper, natural gamma-ray	Caliper and gamma-ray sensor were not calibrated.
Multiparameter	Century Geophysical 8044	Natural gamma-ray, fluid resistivity, spontaneous potential, temperature and change in temperature, 16-in. and 64-in. normal resistivity, single-point resistance, lateral resistivity	Fluid temperature values do not appear valid. Tool likely was stuck at 296 ft (90.2 m) depth despite readings indicating greater depth. Resistivity and spontaneous potential data are noisy. Sensors were not recently calibrated to expected borehole parameters.
Induction	Century Geophysical 9511	Natural gamma-ray, conductivity, resistivity (computed from conductivity)	Sensors were not calibrated. Tool was not calibrated to downhole temperature.
Sonic	Century Geophysical 9320	Natural gamma-ray, full waveform acoustic properties (see Burke, 2011, for details)	Operators could not get the tool past a tight spot at 296 ft (90.2 m) depth, so readings were only acquired above this depth. Gamma-ray sensor was not calibrated.
Neutron	Mount Sopris 2NUA-1000	Neutron	Data are somewhat noisy.
Density	Century Geophysical 9139	Single-arm caliper, natural gamma-ray, bulk density using short and long spacing, compensated bulk density	Caliper and sensors were not recently calibrated to expected borehole parameters.

*Any use of trade, product, or firm names is for descriptive purposes only and does not imply endorsement by the U.S. Government.

operator, we additionally checked the data for depth calibration, applied routines to eliminate spurious data and attenuate noise, adjusted for tool calibration problems, and corrected for effects of borehole fluid and hole diameter. These steps are described in the following sections. Description of the more extensive data processing of the sonic log is described in Burke (2011). Table 5 summarizes the types of processing applied for each log.

Common to the data processing of many of the geophysical logs was the application of spike-rejection and low-pass filters, as implemented by Geosoft OASIS for a sequence of evenly spaced data points. Data spikes were removed using a nonlinear filter, based on a procedure described by Naudy and Dreyer (1968). The filter rejects data points that exceed a particular amplitude tolerance over a certain specified depth interval and replaces them with an estimate based on

Table 4. Description of geophysical logs and their utility for BP-3-USGS.

[PVC, polyvinyl chloride]

Log type	Parameters measured	Physical parameters inferred	Notes important for lithologic interpretation of BP-3-USGS
Caliper	Hole diameter	Wash-outs or restrictions of the sides of the hole	Integrity of the well bore gives clues regarding sand versus clay intervals. Geophysical measurements in wash-outs may be affected and not representative of the formation.
Natural gamma	Natural-gamma radiation	Clay or feldspar content	Radiation increases with increasing clay or increasing potassium associated with abundance of feldspar, such as in volcanic sands. Readings are attenuated inside PVC casing.
Normal resistivity	Electrical resistivity of formation plus pore and borehole fluids, measured over sensor spacings of 16 in. and 64 in.	Lithology, bed boundaries, and water quality	Resistivity generally decreases with increasing clay content. The 64-in. (long-normal) sensor samples greater volume of material vertically and laterally into the formation than does the 16-in. (short-normal) sensor, resulting in a 64-in. normal curve that is much smoother than the 16-in. normal curve. Readings are affected by borehole fluid and are not valid inside the PVC casing.
Induction	Conductivity induced from electromagnetic fields	Lithology and bed boundaries	Resistivity curves computed as the inverse of conductivity data are complimentary to the normal resistivity curves and provide similar information. Readings are unaffected by PVC casing and are more impervious to borehole effects than the normal resistivity sensors.
Spontaneous potential	Natural electrical potentials	Lithology, bed boundaries, and water quality	Curve inflections correspond to contacts between beds of different lithology. Readings are not valid inside PVC casing.
Sonic	Travel time of an acoustic wave between transmitters and receivers	Sonic velocity and porosity	The sonic tool was chosen for BP-3-USGS to get a general sense of the overall sonic velocity of poorly consolidated sediments in this region. The readings are attenuated inside PVC casing.
Neutron	Neutrons slowed and scattered by hydrogen	Saturated porosity	Increasing counts correspond to increasing volume of fluid-filled pore spaces. Porosity and pore connectivity commonly reflect differences in lithology. Clays may have higher porosity than sands, but the pores are not connected, so the effective porosity is low. The readings are attenuated inside PVC casing.
Density	Scattered and attenuated gamma photons	Bulk density and porosity	The density tool was chosen for BP-3-USGS to get a general sense of the overall bulk density of poorly consolidated sediments in this region. The readings are attenuated inside PVC casing.

surrounding data points. We chose amplitude tolerances of about 1.33 percent of the total range of data values and used a depth interval that spans three data points, or an interval of 0.3 ft (9 cm). Low-pass filters were applied to smooth the data, using a convolution filter as described by Fraser and others (1966). The low-pass filter is designed to remove all features of the log trace that have wavelengths less than a designated cutoff wavelength. The filter is tapered using a taper length equal to the wavelength cutoff distance so that side effects of the filtering are minimized. For the BP-3-USGS geophysical logs, we used a wavelength cutoff that spans 20 data points, or a depth interval of 2 ft (0.61 m), except for the normal resistivity logs where a wavelength cutoff spanning 10 points, or a depth interval of 1 ft (0.30 m), was applied.

Check of Depth Calibration

Although natural gamma-ray logs are commonly used to distinguish different lithologies, comparing gamma-ray logs from multiple runs can also help evaluate calibration of depth between logs. Although the amplitudes and details of the gamma-ray curves in counts per second (cps) are expected to vary for each run of the different tools, general features should line up if depth is calibrated correctly. Figure 8 compares the three-arm caliper log and low-pass-filtered, natural gamma-ray logs from five different tools. The caliper records the diameter of the hole through which the tool passed to identify tight spots and wash-outs. Two wash-outs apparent from the wide excursions of the caliper measurements at 80 ft (24.4 m) and 130 ft (39.6 m) are accompanied by abrupt drops in all the gamma-ray curves. Although the wash-outs indicate the geophysical tools were not correctly measuring parameters of the lithology, the drop-outs in the gamma readings are well aligned, indicating that the depth scales on these logs are well calibrated.

The overall shapes of the gamma-ray curves are well matched throughout most of the length of the well confirming that depth is well calibrated between logs. One exception comes from comparing the curves for depths below the tight spot at 296 ft (90.2 m) where the caliper reading reaches less than 4 in. (10 cm). Operators had difficulties getting most of the tools below this point; they abandoned attempts for the sonic tool. However, the multiparameter tool may not have reached the bottom of the hole as well, as evident below this point from a moderate decrease in tension (downloads directory), a lack of character in the multiparameter gamma-ray curve, and flat-lined resistivity readings (not shown). These observations suggest that the multiparameter tool was stuck at this tight spot. Therefore, data were eliminated from the logs appropriate to where each of the sensors was located on the probe when it reached 296 ft (90.2 m).

Because the neutron tool did not include a natural gamma-ray detector, the neutron log was compared to the induction and SP logs to check depth calibration (fig. 9). After application of spike-rejection and low-pass filters to all three logs, many individual features of these curves were similar or mirror images of each other and thus should occur at the same depth. Instead, characteristic features of the neutron curve, indicated at several places on figure 9 by the dashed lines that cross all three logs, appear to be shifted in depth. Because the neutron tool was the only model produced by Mount Sopris rather than Century Geophysical (table 3), the depth offset of the neutron curve may be due to differences in the coefficient

Table 5. Overview of data processing steps applied to geophysical logs.

[PVC, polyvinyl chloride]

Log type	Data editing	Filters applied	Corrections applied
Three-arm caliper	None	None	Shifted to match expected readings inside PVC casing, which has fixed diameter.
Natural gamma (five different tools)	None	Low-pass	None.
Normal resistivity	Remove data measured within PVC casing and depths at bottom, below where the tool was stuck	Spike-rejection and low-pass	Corrected for borehole effects.
Resistivity from induction	None	Low-pass	Scaled to 16-in. normal resistivity curve.
Spontaneous potential	Remove data measured within PVC casing	Spike-rejection and low-pass	None.
Sonic	None	See Burke (2011)	See Burke (2011).
Neutron	None	Spike-rejection and low-pass	Rescale depth to match other tools.
Density	None	Low-pass	Calibration correction.

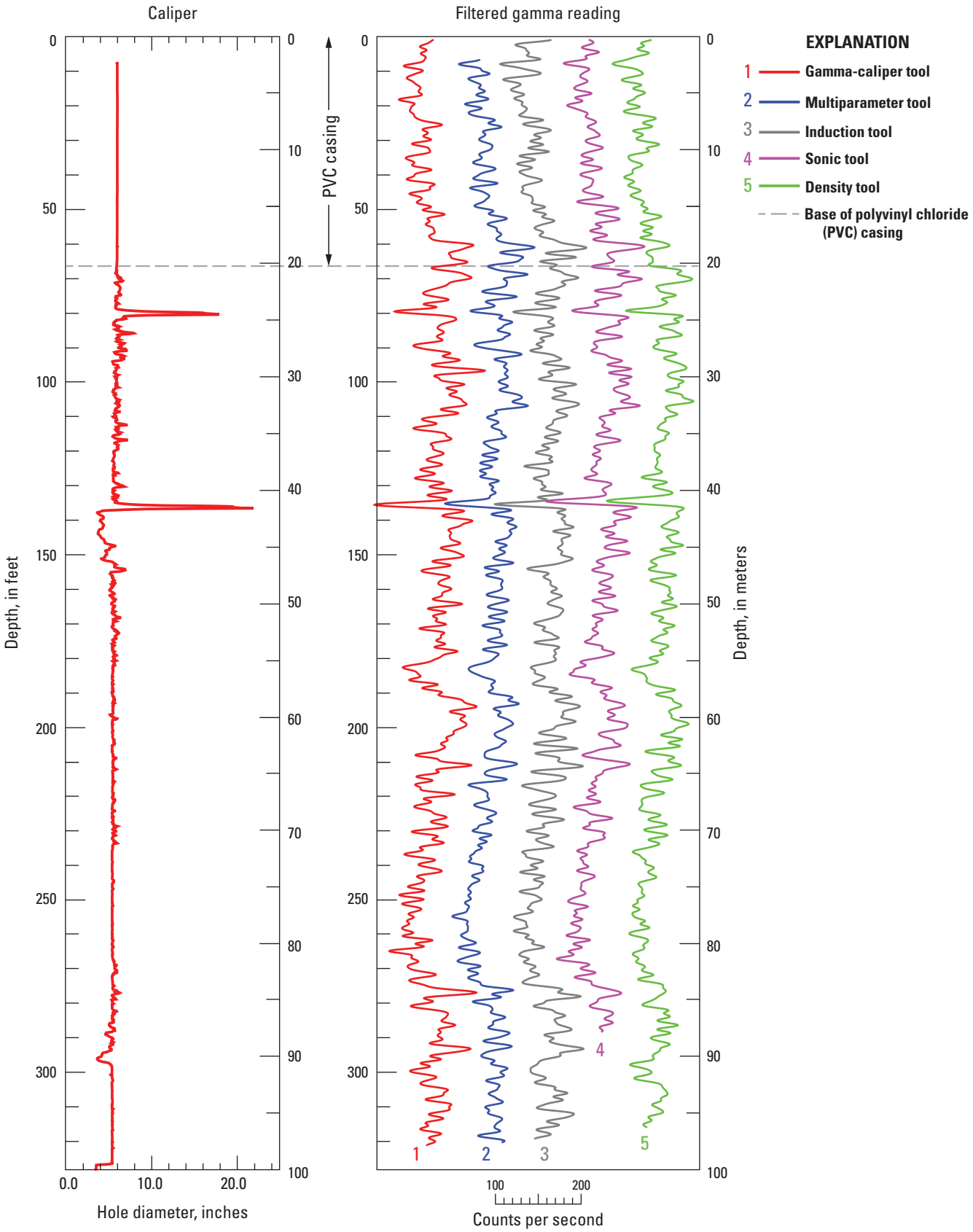

Figure 8. Borehole diameter measured by the three-arm caliper and low-pass-filtered, natural gamma-ray curves from five different tools. Note that the curves are stacked using a relative scale; their absolute values are floating.

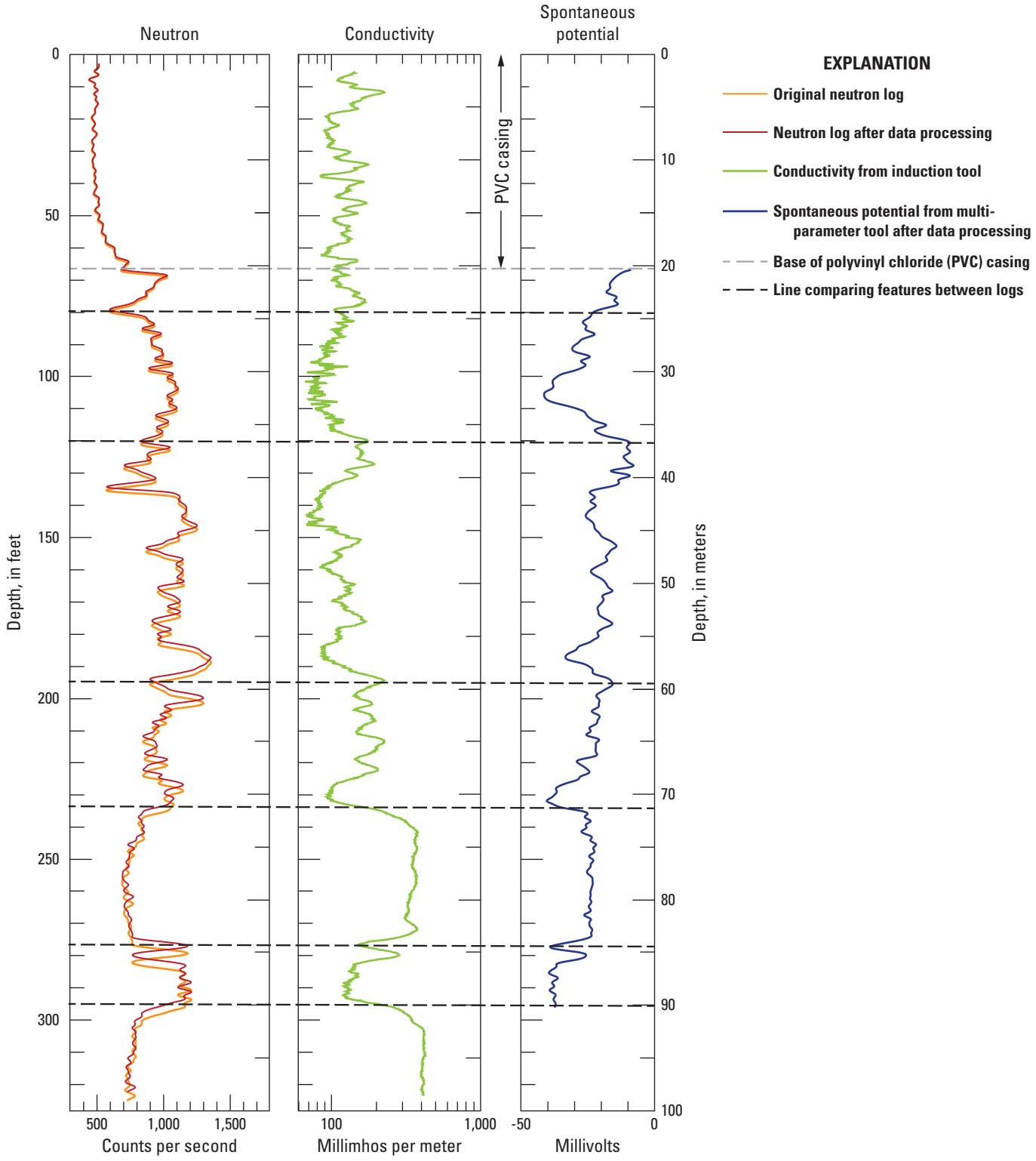

Figure 9. Comparison of original neutron curve to induction and spontaneous potential (SP) logs to correct the depth scale for the neutron log. Characteristic features in the latter two logs were correlated to mirror-image features in the neutron log (correlation across the dashed lines) to determine how depths needed to be scaled. After depth scaling, the characteristic features align much better.

values used by the two companies to determine depth from the number of rotations of the wire reel. A scaling factor of 0.992, determined by inspection, was multiplied to the depth values of the neutron log to fix the problem. The neutron curves before (orange line) and after (red line) correcting the depth scale are shown on figure 9.

Normal Resistivity Logs

Normal resistivity logs need to be corrected for borehole effects to obtain more representative measurements of the resistivity of the formation. Borehole effects include the resistivity of the drilling fluid, borehole diameter, volume of fluid invasion, and bed thickness (Keys, 1990, 1997). Scott (1978) presented a practical algorithm for correcting normal resistivity log data for borehole diameter and mud resistivity. The algorithm is derived from resistivity departure-curve charts developed earlier by Schlumberger Well Surveying Corporation, assuming no invasion of drilling mud and an infinite bed thickness. The validity of these assumptions is difficult to ascertain for BP-3-USGS, but they likely are not met. The correction was applied anyway, assuming it improves the results more than no correction at all.

Figure 10 shows the normal resistivity curves before and after correction and filtering. The correction used equation 2 of Scott (1978), incorporating a tool diameter of 2.1 in. (5.3 cm) and fluid resistivity values taken from those measured during the logging. Resistivities of the fluid varied little throughout the hole, ranging from 5.9 to 6.2 ohm-meter (ohm-m). The fluid was probably well distributed throughout the hole because of the artesian flow. Spike-rejection and low-pass filters were then applied to the corrected normal resistivity data. The low-pass filter used a wavelength cutoff spanning 10 data points (or a depth interval of 1 ft, 0.3 m).

Induction Log

Conductivity readings from the induction tool were inverted to resistivity values for comparison to the normal resistivity logs (fig. 11). The resulting resistivities appeared much too low, likely due to tool calibration problems. On the other hand, individual features of the induction curve show remarkable similarity to the 16-in. normal resistivity curve. Scatter plots comparing resistivity values for the two curves show a linear relation below 120 ft (36.5 m) but no observable relation shallower than this depth. Thus, to adjust for the calibration problem, the induction-tool resistivity values were scaled using a match to the 16-in. normal curve below 120 ft (36.5 m) depth as the criteria. The resulting transform applied to the induction-tool resistivity R_{ind} to get a corrected R_{corr} was computed in ohm-meters as

$$R_{corr} = 3.75\ R_{ind} + 3.3.$$

Figure 11 shows the resistivity curves from the induction tool before and after scaling and after a low-pass filter was applied. The curves are shown in comparison to the normal resistivity curves after they were corrected and filtered.

Why the induction-tool resistivities and the normal resistivities have no apparent relation shallower than 120 ft (36.5 m) is unknown. Resistivities derived from a time-domain electromagnetic (TEM) sounding that was measured at the site before drilling suggest the problem lies with the induction log (fig. 12). The TEM model (D.V. Fitterman, USGS, unpub. data, 2009) is derived by assuming there are only four layers of different resistivity in the subsurface. The resistivities of each model layer, depicted by the straight vertical lines on figure 12, are a broad representation of the resistivities of the formation and pore fluids together. The TEM model matches the borehole resistivity curves fairly well below the depth of 120 ft (36.5 m). The TEM model matches the normal resistivity curves better than the induction-tool resistivity curve above this depth. Interestingly, the 120-ft depth is close to the top of the confining clay layer at 119 ft (36.3 m), suggesting that the explanation is related to differences in the formation fluids in the unconfined and confined aquifers. However, this line of reasoning is contradicted by considering that borehole fluid affects the normal resistivity measurements more than those of the induction tool (table 4).

Density and Sonic Logs

After reviewing the original readings from the two density sensors (short-spaced and long-spaced), it was determined that density values were too low for the known lithology, and the tool calibration was not accurate. In 2013, the two sensors were calibrated at the USGS Texas Water Science Center in Austin, Texas, by measuring two reference blocks with known densities (aluminum and nylon with densities of 2.62 grams per cubic centimeter [g/cm^3] and 1.24 g/cm^3, respectively). This new calibration was then applied to the original log to provide an accurate, compensated bulk density log. A low-pass filter was applied to the compensated density log resulting from the calibration, which is shown in figure 13 alongside the sonic (seismic P-wave) velocity derived from the full waveform sonic log by Burke (2011). These density and sonic logs are best used to provide average values of bulk density and sonic velocity for shallow sediments of the San Luis Valley as opposed to detailed information about variations in lithology in the well. Sonic velocities average 5,922 ft/s (1,805 m/s) (Burke, 2011), with a standard deviation of 230 ft/s (70 m/s). The average and standard deviation from the compensated density log, not considering excursions at 80 and 135 ft (24.4 and 41.4 m) and values measured within the PVC casing, are 1.97 g/cm^3 (1,970 kilograms per cubic meter [kg/m^3]) and 0.12 g/cm^3 (120 kg/m^3), respectively. These measurements are compatible with Gardner's empirical relation between sonic velocity and bulk density in sedimentary basins (Gardner and others, 1974), in which a sonic velocity of 5,922 ft/s (1,805 m/s) relates to a density of 2.02 g/cm^3 (2,020 kg/m^3).

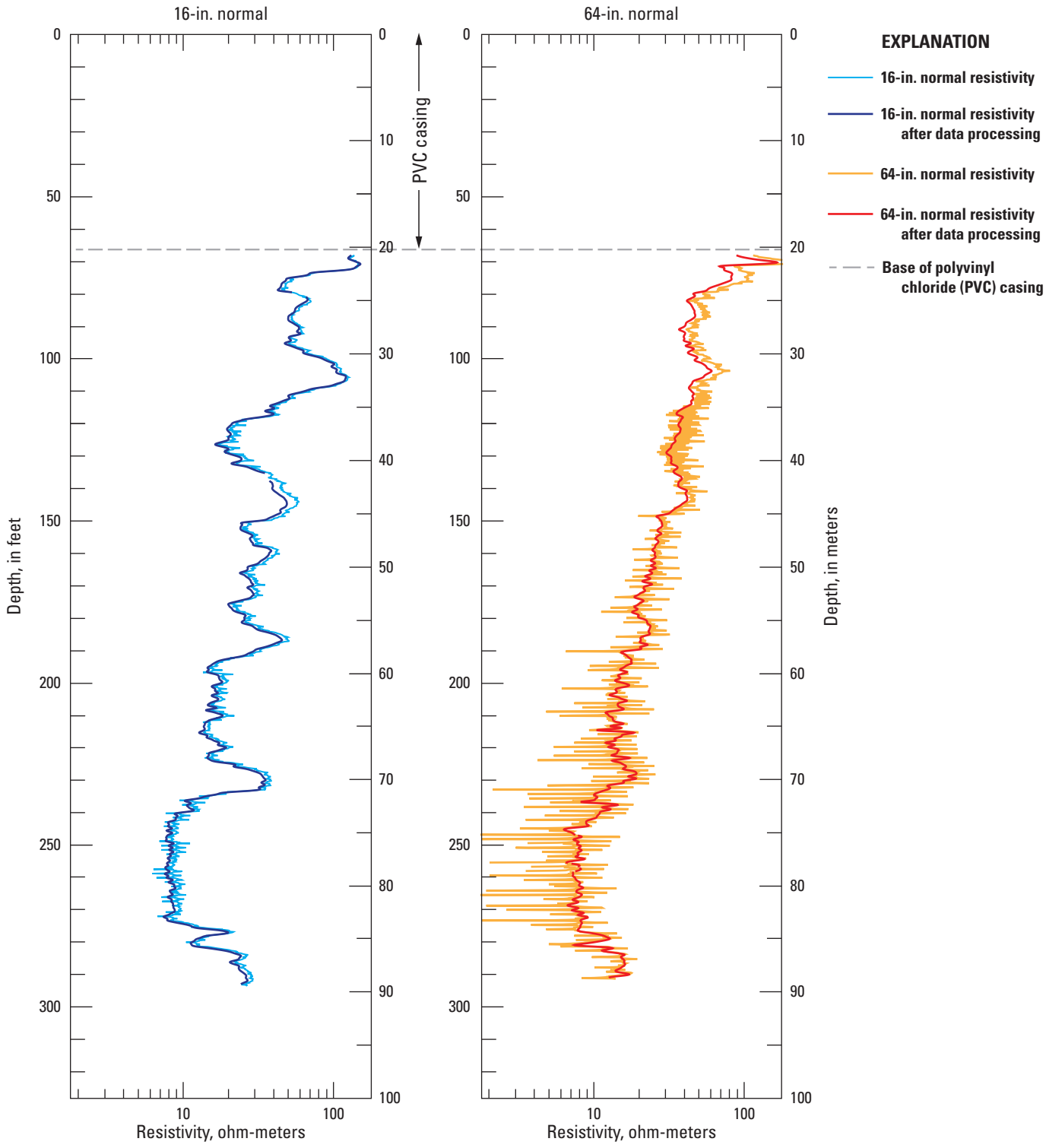

Figure 10. Normal resistivity curves from the multiparameter tool before and after data processing. Normal resistivities were corrected for borehole parameters, then spike-rejection and low-pass filters were applied.

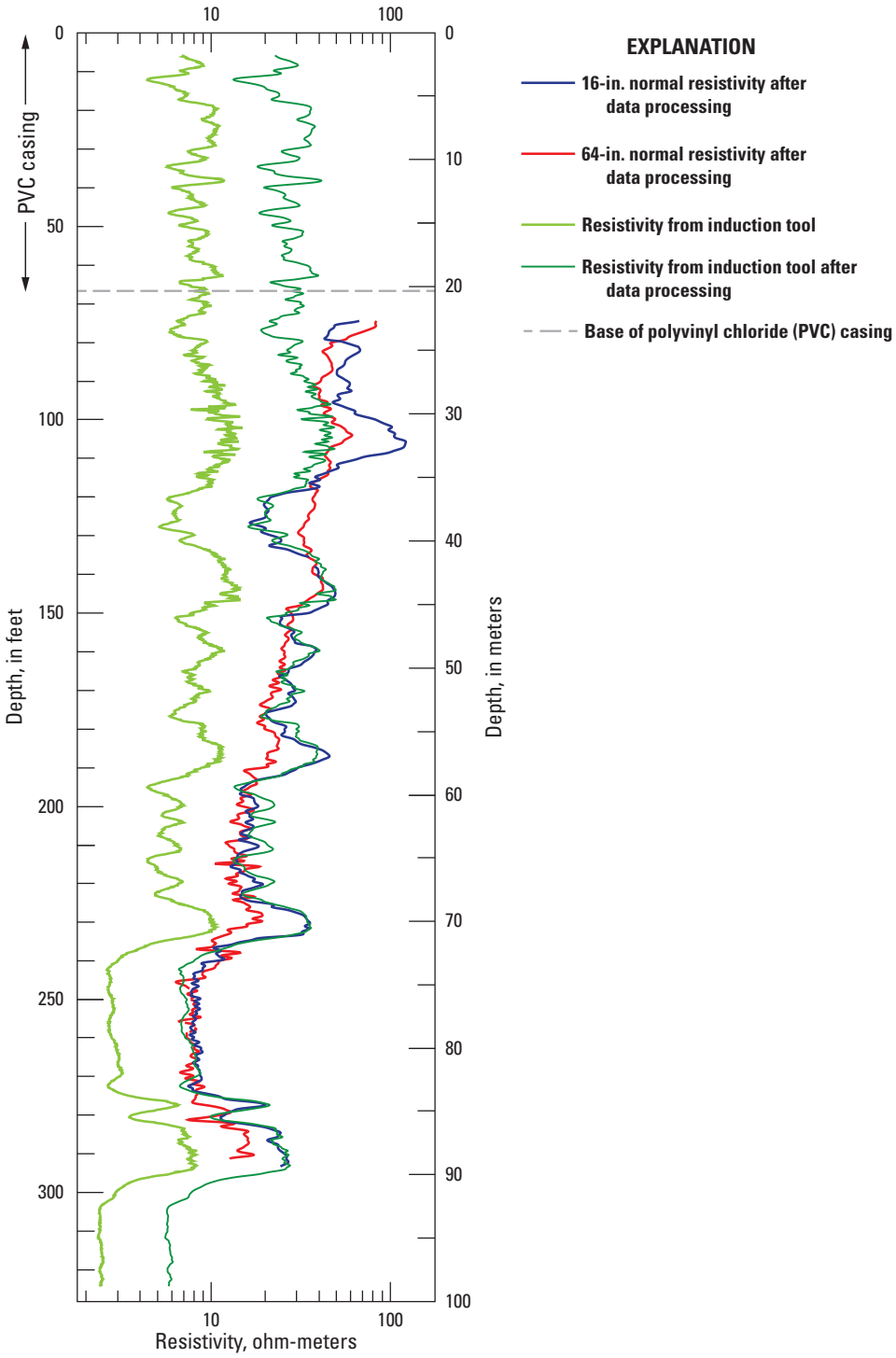

Figure 11. Resistivity derived from the induction tool before and after data processing compared to normal resistivity curves after data processing. The induction-tool resistivity curve was scaled to the 16-in. normal resistivity curve.

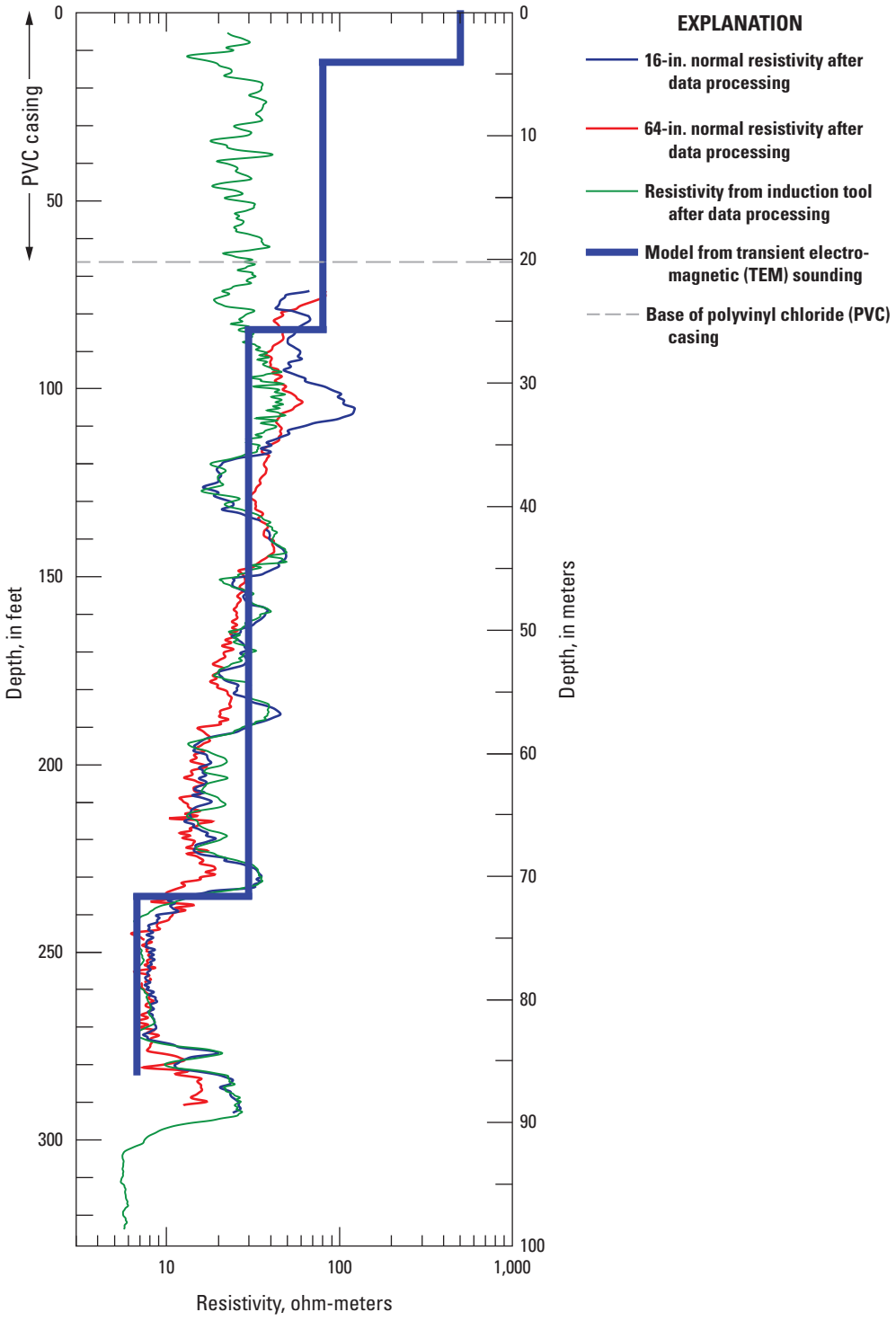

Figure 12. Resistivity curves after data processing compared to resistivity layers derived from a time-domain electromagnetic (TEM) sounding measured at the site before drilling (D.V. Fitterman, U.S. Geological Survey, unpub. data, 2009). The TEM model is derived by assuming there are only four layers of different resistivity in the subsurface.

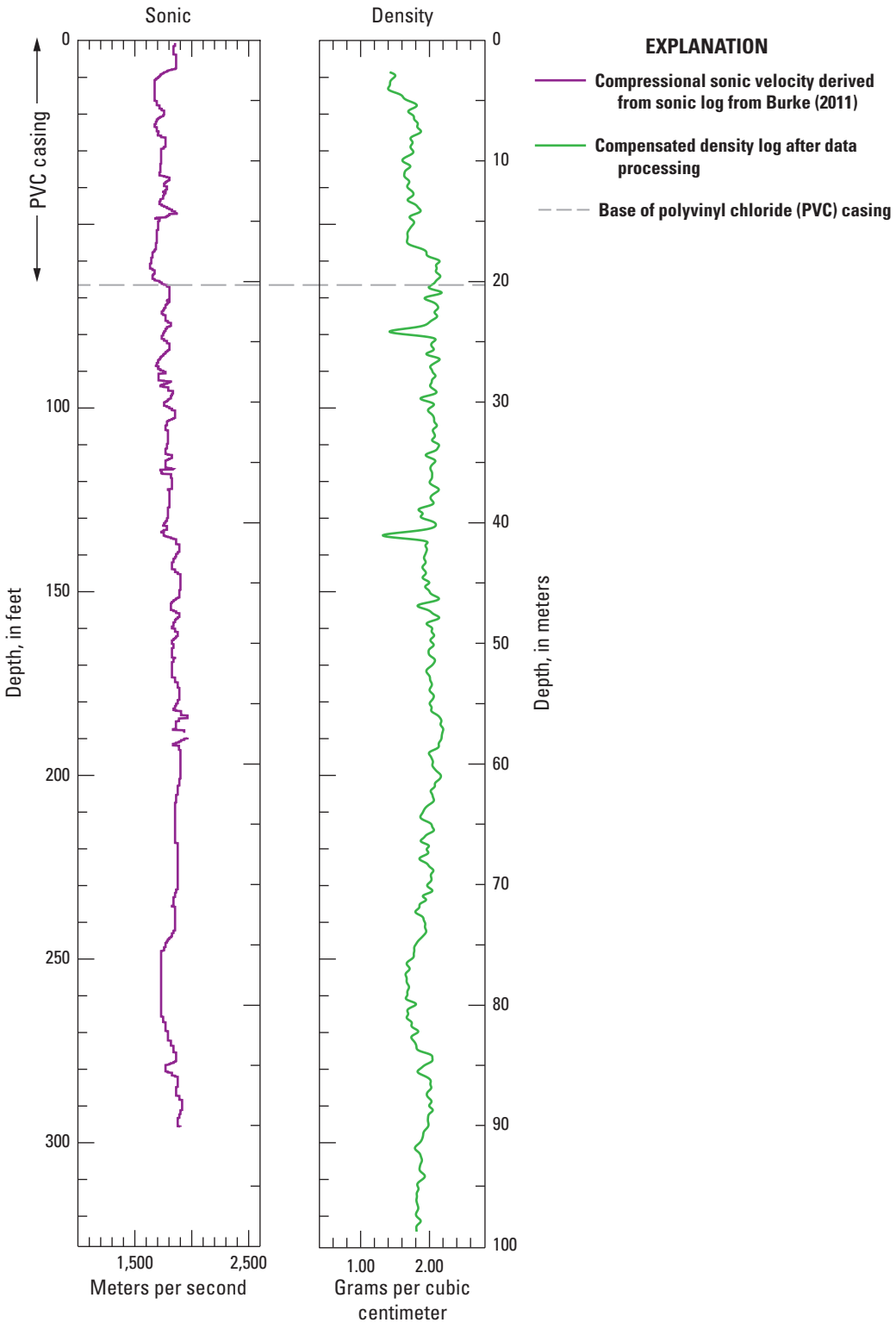

Figure 13. Sonic velocity and compensated density logs.

Digital Log Files

Digital files containing the final, processed data measured by the six borehole tools are available in American Standard Code for Information Interchange (ASCII) format, in the Downloads folder. The data files follow the Log ASCII Standard (LAS) for well logging established by the Canadian Well Logging Society (2011). The files can be read directly by many standard well logging software packages, imported into spreadsheet formats, or opened as an ASCII text file.

Summary of Findings

To serve as a foundation for future research using BP-3-USGS, we developed a generalized lithologic log and selected those borehole geophysical logs that demonstrate the most significant variations to use in comparison (fig. 14). The sample descriptions and their inferred depth positions in the well (fig. 7; appendix 1) were combined with general pattern changes observed mainly in the resistivity (16-in. normal and derived induction-tool logs), gamma-ray, neutron, and SP logs (figs. 8–11) to generalize the lithology across intervals greater than 1 foot. Uncertainties and limitations in determining the lithology with depth vary widely according to the conditions encountered during drilling, sampling, logging, and prolonged storage. These problems, and unresolved problems with calibrations of the resistivity data in particular, are described in detail in previous sections. The uncertainties and limitations suggest the positions of lithologic contacts on the interpreted generalized log are approximate but still adequate to represent a general view of the lithologic variations in the well.

Overall, the generalized lithologic log shows three main packages: (1) mostly sand from the surface to about 77 ft (23.5 m) depth; (2) interbedded sand, silt, and clay decreasing in overall grain size downward from 77 to 232 ft (23.5 to 70.7 m) depth; and (3) thick intervals of massive clay alternating with fine sand to silt from 232 to 326 ft (70.7 to 99.4 m) depth, which is the total depth of the well. Because artesian flow was observed only after drilling through the base of a clay-rich layer within the second lithologic package from 119 to 134 ft (36.3 to 40.8 m) depth, we infer that the base of this clay-rich layer marks the top of the confined aquifer at an elevation of 7,415 ft (2,260 m) above sea level.

The top 77 ft (23.5 m) of mostly sand is compatible with the history of an alluvial-fan environment followed by eolian deposition after the disappearance of Lake Alamosa. The contact between eolian and alluvial-fan deposits, which has been observed in wells elsewhere (Madole and others, 2008), is not well defined from our lithologic descriptions (appendix 1). Observations of mature, well-sorted sand observed from 0 to 20 ft (0 to 6 m) depth and poorly sorted, dominantly coarse-grained sand at 40 ft (12 m) depth (appendix 1) suggest that the contact lies somewhere between 20 and 40 ft (6 and 12 m) depth.

The middle lithologic package, between 77 to 232 ft (23.5 to 70.7 m) depth, is represented by a heterogeneous mix of clastic sediments with a wide range of grain sizes (fig. 14), although grain sizes are generally finer below 150 ft (46 m) than above this depth. The lithologic heterogeneity is mimicked by the large variability in the curves of the borehole logs (fig. 14). A general decrease in grain size with depth is supported by an overall decrease in resistivity. Two thick clay-rich layers at 77–80 ft (23.5–24.4 m) and 119–134 ft (36.3–40.8 m) are actually a mixture of clay and coarser grained material (appendix 1). The well began flowing after drilling had penetrated the base of the deeper clay-rich interval. Freshwater fossils and evidence of bioturbation are common in the clay-rich layers found throughout this lithologic package. Notable is the occurrence of lacustrine diatoms in the topmost clay-rich layer (fig. 14; appendix 2), suggesting that even the youngest deposits of this package accumulated in a lacustrine environment. The interbedded heterogeneous nature of this succession and the relative abundance of freshwater fossils are compatible with the history of a transitional Lake Alamosa that was expanding and contracting before it completely disappeared. Alternatively, the heterogeneity could represent an environment of intermittent lake development that was localized near the well site, especially in the interval above 150 ft (45.7 m). A calcite-cemented sand layer at 181–191 ft (55.2–58.2 m) might represent one of the laterally extensive, poorly cemented sand layers described by Brister and Gries (1994), which they interpret as marking the beginning of the demise of Lake Alamosa.

The clay layer encountered at 232 ft (70.7 m) depth marks the top of the lowermost lithologic package, which is dominated by thick clay layers and intervening fine sand to silt. The blue tint to this clay and to clay in the interval from 254 to 276 ft (77.4 to 84.2 m) suggests one or both of these layers represent the blue clay that is observed in water wells throughout the San Luis Valley. However, this blue clay does not correspond to the top of the confined aquifer that is sometimes presumed elsewhere in the valley (Huntley, 1979a). The blue tint of the top two clay intervals was notably different from the more even gray color of the lower clay interval below 294 ft (89.6 m) when observed in the field, evident now only from photographs (fig. 6). The variation in color may indicate a difference in the chemistry of the depositional environments. Abundant fossils in all the clay layers of the lowermost lithologic package attest to a thriving lacustrine environment, which likely received debris from animals and plants that lived on land nearby. The intervals of sand deposition at well depths of 276–295 ft (84.1–89.9 m) and possibly 241–254 ft (73.5–77.4 m) may represent shifts in the position of the lake basin that persisted for significant periods of time.

Several apparent discrepancies between the borehole logs and the generalized lithologic log, which have different implications, are evident upon examination of figure 14. First, the resistivity values derived from the induction tool appear to be too low in comparison to what is expected for the dominantly sand intervals above 120 ft (36.6 m). For example, coarser grained sand intervals containing fresh water in the upper part

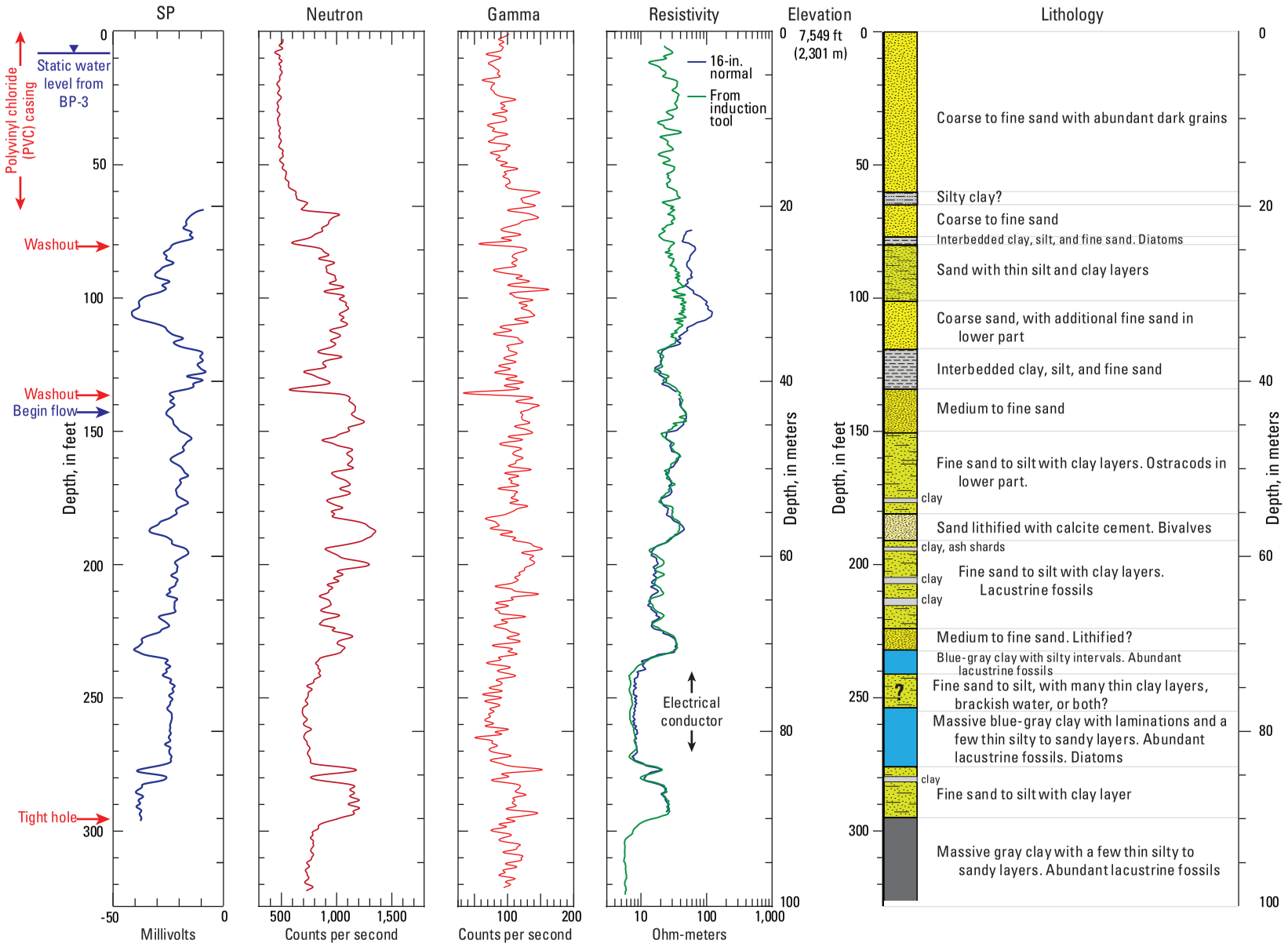

Figure 14. Selected geophysical logs and generalized lithologic log for BP-3-USGS. Only clay layers thicker than 1 ft (0.3 m) are depicted. Water flowing out of the drill stem was observed once the clay-rich layer between depths of 119 and 134 ft (36.3 and 40.8 m) had been penetrated (labeled "Begin flow").The well continued to flow as drilling continued below this depth (fig. 2*E*), but the flow was not measured nor water sampled. The static water level is inferred from neighboring well BP-3 (HRS Water Consultants, Inc., 2009). The top of the interval labeled "Electrical conductor" corresponds to the depth of a conductive layer, similar to that detected in geophysical surveys throughout the region. Uncertainties about the lithology inferred within depth interval 241–254 ft (73.5–77.4 m) are discussed in the text.

of the well (for example, 10–50 ft [3.0–15.2 m]) should have higher resistivities than those with finer grained sand lower in the well (for example, 282–295 ft [86.0–89.9 m]) rather than about the same resistivities, as indicated by the induction-tool resistivity curve (green curve on the resistivity panel of fig. 14). This problem has already been noted in comparison to the normal resistivity logs, but the normal resistivity logs cannot be compared above 67 ft (20.4 m) where the well is cased. For readings above 67 ft (20.4 m), the predominance of sand in well samples supports the supposition that the induction-tool resistivities are also too low above 67 ft. Thus, the induction-tool resistivities should not be used to characterize the resistivities of the lithologies within the entire interval from the surface to 120 ft (36.6 m) depth. Interestingly, the top of the confining clay layer occurs near the problem depth of 120 ft (36.6 m), suggesting that the issues with the induction-tool data somehow correspond to the extent of the unconfined aquifer. However, understanding a physical relation for this correspondence remains elusive.

Second, the gamma-ray log shows apparent discrepancies with the generalized lithologic log. The patterns of the log curve do not have good correlation to variations in clay versus sand and are generally high throughout the well. Commonly, high gamma values correspond to clays and low values to sands (Keys, 1990, 1997; table 4). For example, gamma-ray values within the depth interval 119–150 ft (36.3–45.7 m) are highly variable but do not show the clear difference in pattern between the clay above and sand below that is evident from the well samples and the other geophysical logs (fig. 14). The discrepancy with the gamma-ray log may be caused by volcanic clasts that are prevalent in sands in this area (Madole and others, 2013). Volcanic clasts likely have abundant potassium feldspar and thus increased radioactivity because of the high potassium content (Keys, 1997).

Finally, a discrepancy between all the geophysical logs and the generalized lithologic log occurs between depths 241 and 254 ft (73.5 and 77.4 m), which has significance for future studies. Fine sand to silt is indicated for all but two thin (a foot or less) layers of clay from the drilling speed and from the accompanying bucket sample for 241–251 ft (73.5–76.5 m) (appendix 1). This presumed sandy interval is sandwiched between the two blue-colored clay layers, suggesting that the geophysical logs should have significantly different character across this interval compared to the clay layers. Instead, the SP, neutron, and resistivity logs do not show significant changes in character across the entire sequence of clays and intervening sand to silt (fig. 14), suggesting the whole interval is mostly clay. The gamma-ray log is highly variable across the whole interval, with no clear pattern differences that match the lithologic contacts. Density and sonic velocity logs show a gradual, very slight decrease across the entire sequence, with a minimum at the middle of the presumed sandy layer (fig. 13). The most striking lack of response to the presumed sandy layer comes from the resistivity curve because variations in these data correlate well to differences in sand versus clay content in most of the rest of the well. Even if one assumes maximum error in the depth positioning of core samples, the base of the clay above and the top of the clay below the presumed sandy layer are well constrained (fig. 7), with no more than 4 ft (1.2 m) of error.

The high conductivity (low resistivity) of the presumed sandy interval at 241–254 ft (73.5–77.4 m) might be explained by (1) water contained within a sandy layer that is high in total dissolved solids, such as salt; or (2) a greater clay content than expected within the interval that did not affect drilling speed and was not captured in the core barrel. The first hypothesis explains the on-site and sampling evidence and the resistivity logs but is contradicted by the responses of the other geophysical logs. The second hypothesis explains the responses of the geophysical logs but is contradicted by inferences made from the drilling speed and lack of recovery of any clay-rich material. Possible support for the first hypothesis is the slight separation between the induction-resistivity log and 16-in. short-normal resistivity curves over this interval (fig. 14) where the induction-tool resistivities show lower values. Because the 16-in. short-normal tool has less penetration and is more affected by drilling fluid than the induction tool (table 4), the lower values in the induction-resistivity log suggest that the formation fluid is more conductive than the drilling fluid, which may indicate saline fluid trapped within this interval. However, water from the confined aquifer in two deep wells located about 7 mi (11 km) to the northeast of BP-3-USGS does not show anomalously high specific conductance nor high sodium levels (Rupert and Plummer, 2004). If instead the second hypothesis is true, it is mainly contradicted by the dominance of sand over clay that was inferred from the drilling speed (appendix 1). Because of the limitations of bucket samples discussed earlier, and the low volume of material returned in the bucket for the interval 241–251 ft (73.5–76.5 m) (appendix 1), evidence of fine sand to silt in the bucket sample may be misleading. Perhaps drilling through multiple, thin clay layers dispersed throughout a fine-grained sandy interval might feel as though the material were mostly sand.

Significance for Future Studies

The unique location and setting of BP-3-USGS allow for future study that can test hypotheses developed from the geophysical studies and address questions about the nature and history of Lake Alamosa. The data from this report, combined with preliminary data from several previous studies, suggest promising directions for determining depositional environment through time, improving the understanding of the nature of the confined aquifer, and allowing for integrated interpretation of the aerially extensive geophysical surveys in the area.

Preliminary paleomagnetic measurements indicate that the core samples record a magnetic reversal near the top of the first blue clay layer, tentatively correlated with the 0.78-Ma Brunhes-Matuyama boundary (Davis and others, 2013). These

findings suggest that ages for other intervals of the well can be extrapolated from this interval by determining reasonable sedimentation rates. Volcanic ash shards found in several intervals should be evaluated for age dating or tephrochronologic correlation to samples of known age. Obtaining ages at these intervals would better establish the chronology of the well stratigraphy, confirm the paleomagnetic results, and allow correlation with similar results from outcrop and core samples studied at Hansen Bluff, 24 mi (38 km) to the south (fig. 1) (Rogers and others, 1992; Machette and others, 2007).

Once age is estimated, more detailed studies of the samples could yield information about depositional environment through time. The strategic approach of the studies might follow that of the Hansen Bluff studies. Variations noted in species of ostracods, pollen, fish, and vertebrates in these studies indicated periods of warm versus cold climate (Rogers and others, 1992), which have potential for correlation with species present within BP-3-USGS. In particular, the warm-climate ostracod species *Limnocythere bradburyi* makes up a coquina at the base of Hansen Bluff near a layer of Bishop Tuff ash (Rogers and others, 1992), which has an age of 774 kilo-annum (ka) (Sarna-Wojcicki and others, 2000). *L. bradburyi* was also identified in the blue clay at a depth of 93 m in a deep water well 7 mi (11 km) to the northeast of BP-3-USGS (reported in Madole and others, 2013). If this species is also identified in the blue clay of BP-3-USGS, depositional environment might be correlated across a wide area. If the timing of these variations in environment can be estimated, the findings will have implications for geologic and climatic history for the San Luis Valley. Correlations with worldwide events and geologic mapping of the Rio Grande rift may lead to conclusions about the role of climate versus tectonics during geologic history.

Investigations of BP-3-USGS can also test hypotheses about when and how Lake Alamosa dried up after breaching its lava dam at about 440 ka (Machette and others, 2013). In question is whether sediments from depths of 77–119 ft (23.5–36.3 m), which lie above the confining clay layer, represent transgressions and regressions of Lake Alamosa or whether they were deposited in a local setting with less significance, such as a fluvial environment with migrating oxbow lakes. Preliminary examination of diatoms in the shallow clay layer at 77 ft (23.5 m) depth (fig. 14; appendix 2) indicates a strong presence of a species resembling *Aulacoseira distans* that is known to inhabit small, acidic lakes (Florin, 1981; Camburn and Kingston, 1986; Haworth, 1988; Siver and Kling, 1997; Camburn and Charles, 2000). The genus *Stephanodiscus* was also observed in the clay layer, which is a common planktonic form in lakes, ponds, and large rivers (Stoermer and Julius, 2003). Combined with age estimates, these findings may provide evidence for a revised time frame for the demise of Lake Alamosa.

Diatoms were anticipated in a number of other intervals throughout the core; a few were sampled (appendix 2). One additional interval that yielded diatoms was the blue clay at 261–266 ft (79.6–81.1 m) depth. Preliminary examination of a sample from this interval revealed not only specimens resembling *Aulacoseira distans*, but also a species resembling *Anomoeoneis sphaerophora* f. *costata* that inhabits high-conductance and brackish waters (Kociolek and Spaulding, 2003) and is among species that are prevalent in highly alkaline waters (Schmid, 1977). Additional pennate diatoms were also observed. Though appearing contradictory as to the suggested nature of the lake setting, the importance of this find is that one could interpret the specimens of *Anomoeoneis* as suggestive of a nearby shoreline habitat that had migrated closer to the borehole location due to lake drawdown. Such evidence could have implications for the paleoclimate, the basin geometry, or the regional tectonics. Because no diatoms were discovered in samples from Hansen Bluff (Rogers and others, 1992), the documented presence of diatoms in the BP-3-USGS core presents a unique opportunity for a more systematic diatom study that could assist with future interpretations of the lake history.

Although BP-3-USGS was not drilled to investigate hydrology, two results are significant or worth further study. First, establishing the top of the confined aquifer adds valuable information for regional groundwater models of the area, given the paucity of wells penetrating the confined aquifer in Great Sand Dunes National Park and Preserve (Rupert and Plummer, 2004). Second, the alternate hypotheses to explain the conflict in geophysical log response across the apparent sandy interval at 241–254 ft (73.5–77.4 m) requires further evaluation. Follow-up work would likely focus on additional processing of the geophysical logs and evaluation of other deep wells in the region because core was not recovered from this interval.

Finally, the three general lithologic packages observed in the well have good correspondence to the resistivity model determined from the time-domain EM sounding acquired before drilling (fig. 12). A resistive (>80 ohm-m) layer above 85 ft (25.9 m) depth corresponds well to the upper package of mostly sand, with the uppermost, very resistive 15 ft (4.6 m) perhaps representing unsaturated sand. A 20-ohm-m model layer extending from 85 to 235 ft (25.9 to 71.6 m) corresponds well to the middle interbedded sand, silt, and clay package. Most importantly, the low resistivities (high conductivities) of the lowermost model layer, which is also shown by the resistivity logs (fig. 12), mark the top of the lowermost package containing thick clay layers. Similar model resistivity layers have been observed throughout the park and vicinity in both ground-based and airborne EM surveys (Fitterman and Grauch, 2010; Bedrosian and others, 2012). Most notably, BP-3-USGS supports the hypothesis that the persistent, strong electrical conductor observed in the geophysical surveys corresponds to the top of the first observance of massive blue clay. This confirmation allows future studies to use the electrical conductor as a proxy to correlate this regional clay across a much wider area. Moreover, if the low resistivity (high electrical conductivity) of the sandy interval between the two blue clay layers in BP-3-USGS is caused by saline water, locating the electrical conductor from geophysical surveys may also

locate this unusual layer elsewhere, where its nature can be tested.

Acknowledgments

We thank the USGS Central Region drilling and logging team (Art Clarke, Jeff Eman, Steve Grant, Mike Williams, Derek Gongaware, and Barbara Corland) for their expertise, good humor, and invaluable help. We are indebted to Harland Goldstein (USGS) for his critical support in the sampling operations and field work. We thank Andrew Valdez (NPS) and Fred Bunch (NPS) for their help and advice at the drill site. Invaluable assistance was provided by USGS scientists Janet Slate and Mark Hudson in preliminary evaluations of the well samples and Phil Nelson, Bruce Smith, and especially Greg Stanton, in processing the geophysical logs. We are grateful to HRS Water Consultants, who generously provided advice and information. We appreciate the logistical support and collaboration of the Water Resources Division of NPS, in particular, Jim Harte. Finally, we appreciate the funding and moral support for this serendipitous endeavor by the National Cooperative Geologic Mapping Program, especially Randy Orndorff (USGS).

References Cited

Bedrosian, P.A., Grauch, V.J.S., Bloss, B.R., Fitterman, D.V., Abraham, J.D., and Drenth, B.J., 2012, Mapping lacustrine deposits and faults within the east-central San Luis Basin, Rio Grande rift, using airborne electromagnetic surveys [abs.]: Geological Society of America Abstracts with Programs, v. 44, no. 6, p. 79.

Brendle, D.L., 2002, Geophysical logging to determine construction, contributing zones, and appropriate use of water levels measured in confined-aquifer network wells, San Luis Valley, Colorado, 1998–2000: U.S. Geological Survey Water-Resources Investigations Report 02–4058, 58 p.

Brister, B.S., and Gries, R.R., 1994, Tertiary stratigraphy and tectonic development of the Alamosa basin (northern San Luis Basin), Rio Grande rift, south-central Colorado, *in* Keller, G.R., and Cather, S.M., eds., Basins of the Rio Grande rift—Structure, stratigraphy, and tectonic setting: Geological Society of America Special Paper 291, p. 39–58.

Burke, L., 2011, Digital signal processing and interpretation of full waveform sonic log for well BP-3-USGS, Great Sand Dunes National Park and Preserve, Alamosa County, Colorado: U.S. Geological Survey Scientific Investigations Report 2010–5258, 4 p.

Camburn, K.E., and Charles, D.F., 2000, Diatoms of low-alkalinity lakes in the northeastern United States: The Academy of Natural Sciences of Philadelphia Special Publication 18, 152 p.

Camburn, K.E., and Kingston, J.C., 1986, The genus *Melosira* from soft-water lakes with special reference to northern Michigan, Wisconsin and Minnesota, *in* Smol, J.P., Battarbee, R.W., Davis, R.B., and Meriläinen, J.A., eds., Diatoms and lake acidity—Reconstructing pH from siliceous algal remains in lake sediments: Springer-Verlag, Developments in Hydrobiology no. 29, p. 17–34.

Canadian Well Logging Society, 2011, LAS information—Log ASCII Standard (LAS) software: Canadian Well Logging Society Web site, accessed August 19, 2014, at http://www.cwls.org/las/.

Colman, S.M., McCalpin, J.P., Ostenaa, D.A., and Kirkham, R.M., 1985, Map showing upper Cenozoic rocks and deposits and Quaternary faults, Rio Grande rift, south-central Colorado: U.S. Geological Survey Miscellaneous Investigations Map I–1594, 2 sheets, scale 1:125,000.

Davis, J.K., Hudson, M.R., Slate, J.L., and Grauch, V.J.S., 2013, Preliminary magnetic analysis of the USGS BP3 core, Great Sand Dunes National Park, Colorado [abs.]: Geological Society of America Abstracts with Programs, v. 45, no. 7, p. 603.

Emery, P.A., Snipes, R.J., Dumeyer, J.M., and Klein, J.M., 1973, Water in the San Luis Valley, south-central Colorado: Colorado Water Resources Circular 18, 26 p., 10 pls.

Fitterman, D.V., and de Souza Filho, O.A., 2009, Transient electromagnetic soundings near Great Sand Dunes National Park and Preserve, San Luis Valley, Colorado (2006 field season): U.S. Geological Survey Open-File Report 2009–1051, 55 p.

Fitterman, D.V., and Grauch, V.J.S., 2010, Transient electromagnetic mapping of clay units in the San Luis Valley, Colorado: Proceedings of the 23rd Symposium on the Application of Geophysics to Engineering and Environmental Problems (SAGEEP), 2010 Environmental & Engineering Geophysical Society (EEGS) Annual Meeting, April 11–15, 2010, p. 154–164.

Fitterman, D.V., and Labson, V.F., 2005, Electromagnetic induction methods for environmental problems, *in* Butler, D.K., ed., Near surface geophysics, part 1—Concepts and fundamentals: Tulsa, Okla., Society of Exploration Geophysicists, p. 301–355.

Florin, M.-B., 1981, The taxonomy of some *Melosira* species—A comparative morphological study, *in* Ross, R., ed.: II. Proceedings of the 6th International Symposium on Recent and Fossil Marine Diatoms, Budapest, September 1–5, 1980, p. 43–67.

Fraser, D.C., Fuller, B.D., and Ward, S.H., 1966, Some numerical techniques for application in mining exploration: Geophysics, v. 31, no. 6, p. 1066–1077.

Gardner, G.H.F., Gardner, L.W., and Gregory, A.R., 1974, Formation velocity and density—The diagnostic basics for stratigraphic traps: Geophysics, v. 39, no. 6, p. 770–780.

Grauch, V.J.S., Bedrosian, P.A., Drenth, B.J., and Bloss, B.R., 2013, Mapping under the sand—Progress report on geophysical studies in Great Sand Dunes National Park, Colorado [abs.]: Geological Society of America Abstracts with Programs, v. 45, no. 7, p. 67.

Grauch, V.J.S., Fitterman, D.V., Slate, J.L., and Drenth, B.J., 2010, Mapping Plio-Pleistocene lake deposits under Great Sand Dunes National Park, San Luis Valley, Colorado—Insights from recent drilling and geophysical surveys [abs.]: Geological Society of America Abstracts with Programs, v. 42, no. 5, p. 455.

Harmon, E.J., 2010, Hydrogeologic controls by depositional and lithofacies transitions—Great Sand Dunes National Park and Preserve, Colorado [abs.]: Geological Society of America Abstracts with Programs, v. 42, no. 5, p. 454.

Haworth, E.Y., 1988, Distribution of diatom taxa of the old genus *Melosira* (now mainly *Aulacoseira*) in Cumbrian waters, *in* Round, E.F., ed., Algae and the aquatic environment: Bristol, United Kingdom, Biopress, p. 138–167.

Hearne, G.A., and Dewey, J.D., 1988, Hydrologic analysis of the Rio Grande Basin north of Embudo, New Mexico, Colorado and New Mexico: U.S. Geological Survey Water-Resources Investigations Report 86–4113, 244 p., 1 pl.

HRS Water Consultants, Inc., 1999, Hydrogeologic investigation, Sand Creek and Indian Springs area, Great Sand Dunes National Monument, Colorado: Lakewood, Colo., HRS Water Consultants, Inc., Report to National Park Service 92021–04, 40 p.

HRS Water Consultants, Inc., 2009, Documentation of boundary piezometer installation, Great Sand Dunes National Park and Preserve, Colorado: Lakewood, Colo., HRS Water Consultants, Inc., Report to U.S. Department of Justice and National Park Service, December 2009, HRS Project 04-06.10.

Huntley, David, 1979a, Ground-water recharge to the aquifers of northern San Luis Valley, Colorado: Geological Society of America Bulletin, Part II, v. 90, no. 8, p. 1196–1281.

Huntley, David, 1979b, Cenozoic faulting and sedimentation in northern San Luis Valley, Colorado: Geological Society of America Bulletin, Part II, v. 90, no. 1, p. 135–153.

Keys, W.S., 1990, Borehole geophysics applied to groundwater investigations: U.S. Geological Survey Techniques of Water Resources Investigations Book 2, chapter E–2, 150 p.

Keys, W.S., 1997, A practical guide to borehole geophysics in environmental investigations: Boca Raton, Fla., CRC-Lewis Publishers, 176 p.

Kirkham, R.M., and Rogers, W.P., 1981, Earthquake potential in Colorado: Colorado Geological Survey Bulletin 43, p. 171.

Knight, R.J., and Endres, A.L., 2005, An introduction to rock physics principles for near-surface geophysics, *in* Butler, D.K., ed., Near surface geophysics, part 1—Concepts and fundamentals: Tulsa, Okla., Society of Exploration Geophysicists, p. 31–70.

Kociolek, J.P., and Spaulding, S.A., 2003, Symmetrical Naviculoid diatoms, *in* Wehr, J.D., and Sheath, R.G., eds., Freshwater algae of North America—Ecology and classification: New York, Academic Press, p. 637–668.

Machette, M.N., 2007, Chapter B—Field trip day 2—Quaternary geology of Lake Alamosa and the Costilla Plain, southern Colorado, *in* Machette, M.N., Coates, M.-M., and Johnson, M.L., eds., 2007 Rocky Mountain Section Friends of the Pleistocene Field Trip—Quaternary geology of the San Luis Basin of Colorado and New Mexico, September 7–9, 2007: U.S. Geological Survey Open-File Report 2007–1193, p. 53–108. http://pubs.usgs.gov/of/2007/1193/.

Machette, M.N., Marchetti, D.W., and Thompson, R.A., 2007, Chapter G—Ancient Lake Alamosa and the Pliocene to middle Pleistocene evolution of the Rio Grande, *in* Machette, M.N., Coates, M.-M., and Johnson, M.L., eds., 2007 Rocky Mountain Section Friends of the Pleistocene Field Trip—Quaternary geology of the San Luis Basin of Colorado and New Mexico, September 7–9, 2007: U.S. Geological Survey Open-File Report 2007–1193, p. 157–167*, http://pubs.usgs.gov/of/2007/1193/.*

Machette, M.N., Thompson, R.A., Marchetti, D.W., and Smith, R.S.U., 2013, Evolution of ancient Lake Alamosa and integration of the Rio Grande during the Pliocene and Pleistocene, *in* Hudson, M.R., and Grauch, V.J.S., eds., New perspectives on Rio Grande rift basins—From tectonics to groundwater: Geological Society of America Special Paper 494, p. 1–20.

Madole, R.F., Mahan, S.A., Romig, J.H., and Havens, J.C., 2013, Constraints on the age of the Great Sand Dunes, Colorado, from subsurface stratigraphy and OSL dates: Quaternary Research, v. 80, p. 435–446.

Madole, R.F., Romig, J.H., Aleinikoff, J.N., VanSistine, D.P., and Yacob, E.Y., 2008, On the origin and age of the Great Sand Dunes, Colorado: Geomorphology, v. 99, p. 99–119.

Naudy H., and Dreyer H., 1968, Essai de filtrage nonlineare applique aux profils aeromagnetiques: Geophysical Prospecting, v. 16, no. 2, p. 171.

Rogers, K.L., Larson, E.E., Smith, G., Katzman, D., Smith, G.R., Cerling, T., Wang, Y., Baker, R.G., Lohmann, K.C., Repenning, C.A., Patterson, P., and Mackie, G., 1992, Pliocene and Pleistocene geologic and climatic evolution in the San Luis Valley of south-central Colorado: Palaeogeography, Palaeoclimatology, Palaeoecology, v. 94, p. 55–86.

Rogers, K.L., Repenning, C.A., Forester, R.M., Larson, E.E., Hall, S.A., Smith, G.R., Anderson, E., and Brown, T.J., 1985, Middle Pleistocene (late Irvingtonian: Nebrasakan) climatic changes in south-central Colorado: National Geographic Research, v. 1, no. 4, p. 535–563.

Ruleman, C., and Machette, M.N., 2007, An overview of the Sangre de Cristo fault system and new insights to interactions between Quaternary faults in the northern Rio Grande rift, *in* Machette, M.N., Coates, M.-M., and Johnson, M.L., eds., 2007 Rocky Mountain Section Friends of the Pleistocene field trip–Quaternary geology of the San Luis Basin of Colorado and New Mexico, September 7–9, 2007: U.S. Geological Survey Open-File Report 2007–1193, p. 187–197.

Rupert, M.G., and Plummer, L.N., 2004, Ground-water flow direction, water quality, recharge sources, and age, Great Sand Dunes National Monument, south-central Colorado, 2000–2001: U.S. Geological Survey Scientific Investigations Report 2004–5027, 28 p.

Sarna-Wojcicki, A.M., Pringle, M.S., Wijbrans, J., 2000, New $^{40}Ar/^{39}Ar$ age of the Bishop Tuff from multiple sites and sediment rate calibration for the Matuyama-Brunhes boundary: Journal of Geophysical Research, v. 105, no. B9, p. 21,431–21,443.

Schmid, A., 1977, Morphological and physiological examination of diatoms of Neusiedler Lake. 2. Photomicroscopic and scanning electron-microscopic shell analysis of environmentally conditioned cyclomorphosis of *Anomoeoneis-sphaerophora* (KG) Pfitzer: Nova Hedwigia, v. 28, no. 2-3, p. 309–351.

Scott, J.H., 1978, A FORTRAN algorithm for correcting normal resistivity logs for borehole diameter and mud resistivity: U.S. Geological Survey Open-File Report 78–669, 12 p.

Siebenthal, C.E., 1910, Geology and water resources of the San Luis Valley, Colorado: U.S. Geological Survey Water Supply Paper 240, 128 p.

Siver, P.A., and Kling, H., 1997, Morphological observations of *Aulacoseira* using scanning electron microscopy: Canadian Journal of Botany, v. 75, p. 1807–1835.

Stoermer, E.F., and Julius, M.L., 2003, Centric diatoms, *in* Wehr, J.D., and Sheath, R.G., eds., Freshwater algae of North America—Ecology and classification: New York, Academic Press, p. 559–594.

Appendixes

Appendix 1. Descriptions of samples by type and drilling interval.

[Drilling depth interval, interval evaluated for sampling; those sampled for core are indicated by the core run number; depths listed in feet (ft), corresponding to drilling procedures; m, meters. Sample types described in text and table 1. N/A, not applicable. XRD, X-ray diffraction. Analyses are presented in appendix 3. Onsite core recovery length is the original length measured in 2009. Cores are logged from bottom (0.0 ft) to the top of the sample relative to core lengths measured in 2013, which could be different than the onsite length (table 2). See appendix 2 for more detail on fossil and trace fossil observations.]

Drilling depth interval	Description from drilling speed and onsite observations	Descriptions of mud stream samples	Descriptions of core barrel samples
0–20 ft (0–6.1 m) Rotary drilling	Coarse sand with clumps of silty clay	Sieved cuttings at 10 ft. Coarse sand to clay with poorly sorted subrounded to rounded, mostly dark grains. Slightly calcareous. Sieved cuttings at 20 ft. Coarse to fine sand with rounded to subrounded grains. Noncalcareous. Hopper samples (coarse and fine fractions) from 0–20 ft. Coarse to very fine sand with subrounded to rounded, mostly dark grains. About twice the volume of coarse- compared to fine-grained fraction. Very mature. Slightly calcareous.	N/A
20–40 ft (6.1–12.2 m) Rotary drilling	Coarse sand with clumps of green clay grading downward to fine sand	Hopper samples (coarse and fine fractions) from 20–30 ft. Coarse to fine sand with rounded to subrounded, mostly dark grains. Noncalcareous. Sieved cuttings at 30 ft. Coarse to fine sand with rounded to subrounded, mostly dark grains. Noncalcareous. Hopper samples (coarse and fine fractions) from 30–40 ft. Coarse to fine sand with subangular to rounded, mostly dark grains. Noncalcareous. Sample taken from fine fraction for XRD analysis Sieved cuttings at 40 ft. Very coarse to fine sand, dominated by coarse sand. Poorly sorted, subangular to rounded, mostly dark grains, some volcanic grains. Noncalcareous.	N/A

Appendix 1. Descriptions of samples by type and drilling interval.—Continued

[Drilling depth interval, interval evaluated for sampling; those sampled for core are indicated by the core run number; depths listed in feet (ft), corresponding to drilling procedures; m, meters. Sample types described in text and table 1. N/A, not applicable. XRD, X-ray diffraction. Analyses are presented in appendix 3. Onsite core recovery length is the original length measured in 2009. Cores are logged from bottom (0.0 ft) to the top of the sample relative to core lengths measured in 2013, which could be different than the onsite length (table 2). See appendix 2 for more detail on fossil and trace fossil observations.]

Drilling depth interval	Description from drilling speed and onsite observations	Descriptions of mud stream samples	Descriptions of core barrel samples
40–60 ft (12.2–18.3 m) Rotary drilling	Fine to coarse sand with clumps of clay at 60 ft	Hopper samples (coarse and fine fractions) from 40–50 ft. Coarse to fine sand with subangular to rounded, mostly dark grains and some pebbles. Noncalcareous. Sieved cuttings at 50 ft. Coarse to fine sand with subrounded to rounded, mostly dark grains. Slightly calcareous. Hopper samples (coarse and fine fractions) from 50–60 ft. Coarse to very fine sand with subangular to rounded, dark grains. Poorly sorted. Sieved cuttings at 60 ft. Coarse to fine sand with subangular to rounded grains. Some magnetic grains, some volcanic grains, some biotite. Maybe some volcanic glass. Noncalcareous. Hand sample of clay and sand at 60 ft. Coarse to fine sand, subangular to rounded grains, poorly sorted. Not much clay.	N/A
60–70 ft (18.3–21.3 m) Core run 1	Sand with clay from 60–68 ft	N/A	Viscous fluid sample, sieved. Very coarse to fine sand with poorly sorted, subangular to rounded grains. Abundant dark grains. Noncalcareous. Sieving may have removed silts and clays. Support for silty clay in the interval 60–65 ft comes from slight drop in resistivity from induction log and nearby BP-3 well where silty clay was logged from 60–66 ft. Other logs cannot be evaluated because this interval is mostly inside the casing.
70–80 ft (21.3–24.4 m) Core run 2	Sand with clay layer at 77 ft	N/A	Core catcher sample (probably from 77 ft). Very fine sand to silt interbedded with clay. Sand and silt have angular to subrounded, well-sorted grains and tan color, mostly quartz. Not as many dark grains compared to intervals above. Calcareous. Clay is greenish-gray, very calcareous. Some beds are fine sand to clay. Geophysical logs and lithology in neighboring BP-3 well indicate the fine-grained interval extends from 77–80 ft. Two samples taken for XRD analysis. Diatoms.

Appendix 1. Descriptions of samples by type and drilling interval.—Continued

[Drilling depth interval, interval evaluated for sampling; those sampled for core are indicated by the core run number; depths listed in feet (ft), corresponding to drilling procedures; m, meters. Sample types described in text and table 1. N/A, not applicable. XRD, X-ray diffraction. Analyses are presented in appendix 3. Onsite core recovery length is the original length measured in 2009. Cores are logged from bottom (0.0 ft) to the top of the sample relative to core lengths measured in 2013, which could be different than the onsite length (table 2). See appendix 2 for more detail on fossil and trace fossil observations.]

Drilling depth interval	Description from drilling speed and onsite observations	Descriptions of mud stream samples	Descriptions of core barrel samples
80–90 ft (24.4–27.4 m) Core run 3	Coarse sand with a little hard, dark clay	N/A	Core catcher sample (possibly from 85 ft, based on geophysical logs). Very fine sand to clay, mostly silt with very little coarse sand. Well-sorted angular to subangular grains. Fewer dark grains than above, some mica. Noncalcareous. Sample taken for XRD analysis.
90–92 ft (27.4–28.0 m) Core run 4	Dark-gray silty clay and fine sand with layer-like chunks of lime-green clay	Sieve sample at 92 ft. Coarse to fine sand, angular to rounded grains, poorly sorted. Some mica, one large potassium feldspar grain. Very calcareous.	Core catcher plus viscous fluid samples, sieved. Very fine sand to silt, some coarse sand, not much clay, if any. Mostly quartz. Lots of mica. Medium to well sorted. Slightly calcareous.
92–94 ft (28.0–28.7 m) Core run 5	Sand with layer-like chunks of green clay	N/A	Viscous fluid sample, scooped. Medium to very fine sand, subangular to rounded grains. Some clumps of blue clay. Medium sorting. Slightly calcareous. Core catcher sample. Coarse sand to silt, poorly sorted. Mostly quartz grains with some potassium feldspar, relatively few dark grains, some magnetite grains. Very calcareous.
94–96 ft (28.7–29.3 m) Core run 6	Clay above medium, dark gray sand	N/A	Core catcher sample (probably from 94 ft). Fine sand to clay with well-sorted, angular to subrounded grains. Clumps of tan clay. Some clumps of medium sand with darker grains. Noncalcareous.
96–101 ft (29.3–30.8 m) Core run 7	Sand	N/A	Viscous fluid sample, sieved. Coarse to very fine sand with medium-sorted, subangular to rounded dark grains. Noncalcareous. Core catcher sample (probably from 101 ft). Fine sand to silt with very well-sorted, subangular to rounded grains. Moderately abundant dark grains. Noncalcareous.

Appendix 1. Descriptions of samples by type and drilling interval.—Continued

[Drilling depth interval, interval evaluated for sampling; those sampled for core are indicated by the core run number; depths listed in feet (ft), corresponding to drilling procedures; m, meters. Sample types described in text and table 1. N/A, not applicable. XRD, X-ray diffraction. Analyses are presented in appendix 3. Onsite core recovery length is the original length measured in 2009. Cores are logged from bottom (0.0 ft) to the top of the sample relative to core lengths measured in 2013, which could be different than the onsite length (table 2). See appendix 2 for more detail on fossil and trace fossil observations.]

Drilling depth interval	Description from drilling speed and onsite observations	Descriptions of mud stream samples	Descriptions of core barrel samples
101–119 ft (30.8–36.3 m) (No core sample)	Sand with thin layers of clay at 115 ft and 119 ft	Sieve sample at 105 ft. Coarse sand with medium-sorted, subangular to rounded grains. Abundant dark grains. Noncalcareous. Sieve sample at 112 ft. Coarse sand with medium-sorted, subangular to rounded grains. Abundant dark grains. Noncalcareous. Sieve sample at 115 ft. Coarse sand with medium-sorted, subangular to rounded grains. Abundant dark grains. Noncalcareous. Sieve sample at 119 ft. Coarse to fine sand with poorly sorted, subangular to rounded dark grains. Noncalcareous.	N/A
119–125 ft (36.3–38.1 m) Core run 8	Clay with sand gradually increasing downward	N/A	Core piece (1.6 ft fell off core table, probably from 119–121 ft). Fine sand to clay with subangular to rounded grains. Sandy clay interbedded with sand layers. Noncalcareous. Core catcher sample. Fine sand to silt with well-sorted, angular to subrounded grains. Moderately abundant dark grains. Noncalcareous, although light-colored pockets are calcareous. Sample taken for XRD analysis.
125–128 ft (38.1–39.0 m) Core run 9	Clay	N/A	Core (1.0 ft onsite recovery, probably from 125–126 ft). *0.5–1.0* Dark gray silty clay with fewer dark grains in the finer material. Slightly calcareous. *0.0–0.5* Light gray sandy clay. Sand consists of abundant dark grains. Slightly calcareous. Faintly bedded. Dessication cracks parallel to bedding. Core catcher sample. Medium well sorted silt to clay, with very little silt. Some mica. Noncalcareous.
128–131 ft (39.0–39.9 m) Core run 10	Clay changing to sand below 129 ft	N/A	Core catcher sample (probably from 128–129 ft). Fine sand to clay, mostly silt, with medium sorted, subangular to rounded dark grains. Very calcareous.

Appendix 1. Descriptions of samples by type and drilling interval.—Continued

[Drilling depth interval, interval evaluated for sampling; those sampled for core are indicated by the core run number; depths listed in feet (ft), corresponding to drilling procedures; m, meters. Sample types described in text and table 1. N/A, not applicable. XRD, X-ray diffraction. Analyses are presented in appendix 3. Onsite core recovery length is the original length measured in 2009. Cores are logged from bottom (0.0 ft) to the top of the sample relative to core lengths measured in 2013, which could be different than the onsite length (table 2). See appendix 2 for more detail on fossil and trace fossil observations.]

Drilling depth interval	Description from drilling speed and onsite observations	Descriptions of mud stream samples	Descriptions of core barrel samples
131–141 ft (39.9–43.0 m) Core run 11	Interbedded sand and clay, some black nodules (peat?)	Bucket sample, 131–141 ft. Coarse sand to clay, with poorly sorted, angular to subrounded grains. Very few dark grains. Noncalcareous.	Core (0.6 ft onsite recovery). *0.3–0.8* Medium sand to clay, mostly sand; abundant dark grains. Possible bioturbation from 0.7 to 0.8 ft; massive with no laminations elsewhere. Calcareous. *0.2–0.3* Coarse sand to clay, mostly sand. Slightly calcareous. *0.0–0.2* Fine sand to clay, mostly clay; fewer dark grains than above. Slightly calcareous. Core catcher sample (probably from 134 ft, based on geophysical and caliper logs). Fine sand to clay, mostly silt, with medium sorted, subangular to rounded dark grains. Noncalcareous.
141–151 ft (43.0–46.0 m) Core run 12	Sand, with less than 1-ft-thick layers of clay at 145 ft and 151 ft	Bucket sample, 141–151 ft. Medium to fine sand, with well-sorted, subangular to rounded grains. Abundant dark grains. Noncalcareous.	Core catcher sample (probably from 151 ft, based on geophysical logs). Fine sand to clay, with well-sorted, subangular to rounded grains. Clay is calcareous; fine sand is not.
151–161 ft (46.0–49.1 m) (No core sample)	Fine sand with only a little clay	Bucket sample, 151–161 ft. Fine sand to silt, with medium sorted, subangular to rounded grains. Quartz grains more abundant than dark grains. Noncalcareous.	N/A
161–171 ft (49.1–52.1 m) (No core sample)	Fine sand with a few thin clay layers	Bucket sample, 161–171 ft. Fine sand to silt, with medium-sorted, subangular to rounded grains. Quartz grains more abundant than dark grains. Noncalcareous.	N/A

Appendix 1. Descriptions of samples by type and drilling interval.—Continued

[Drilling depth interval, interval evaluated for sampling; those sampled for core are indicated by the core run number; depths listed in feet (ft), corresponding to drilling procedures; m, meters. Sample types described in text and table 1. N/A, not applicable. XRD, X-ray diffraction. Analyses are presented in appendix 3. Onsite core recovery length is the original length measured in 2009. Cores are logged from bottom (0.0 ft) to the top of the sample relative to core lengths measured in 2013, which could be different than the onsite length (table 2). See appendix 2 for more detail on fossil and trace fossil observations.]

Drilling depth interval	Description from drilling speed and onsite observations	Descriptions of mud stream samples	Descriptions of core barrel samples
171–191 ft (52.1–58.2 m) Core run 13	Fine to coarse sand with clay layer at 175–176 ft and apparent clay layers at 180 ft, 187–188 ft, and 189–191 ft. The appearance of light-colored chunks along with higher values on the resistivity and density logs (examined later) suggest that slow drilling speeds were caused by lithified sand rather than clay within 181–191 ft	Bucket sample, 171–181 ft. Fine sand to silt, with medium-sorted, subangular to rounded grains. Quartz grains more abundant than dark grains. Noncalcareous. Bucket sample at 181–191 ft. Fine sand to silt, with medium-sorted, subangular to rounded grains. Very slightly calcareous. Sample of clam shells collected. Hand samples of light-colored chunks at 191 ft. Coarse to fine sand with subangular to rounded grains. Most of the coarse particles are aggregates of fine sand cemented with calcium carbonate.	Core (4.0 ft onsite recovery, but core was in pieces that may not have been contiguous). *3.7–4.0* Abrupt transition at 3.7 ft from muddy sand below to dark greenish-gray clay above. Grades upward from noncalcareous to calcareous. This piece may not be contiguous with core below. *2.7–3.7* Muddy sand. Calcareous. *2.5–2.7* Grades upward from clay to muddy sand. Calcareous. *0.7–2.5* Greenish-gray clay with some silt, possibly from 175–177 ft, based on drilling description and geophysical logs. Calcareous. A few ostracods at 1.7 to 2.0 ft. Rust colored stain in spots at 2.3 ft probably developed during sample storage. *Some core sample is presumed missing here. Assume core above and below are not contiguous based on attempts to match lithologies with geophysical logs.* *0.0–0.7* Coarse to medium, light tan, very well sorted, fairly clean sand with calcareous cement. Faint laminations may have been caused by coring bit. Grades upward into clay. Probably from somewhere near the top of 186–191 ft from driller's observations and geophysical logs. Core catcher sample (probably from 191 ft based on hand collected sample. Fine sand to silt, with well sorted, subangular to rounded grains. Lithified with very calcareous cement.

Appendix 1. Descriptions of samples by type and drilling interval.—Continued

[Drilling depth interval, interval evaluated for sampling; those sampled for core are indicated by the core run number; depths listed in feet (ft), corresponding to drilling procedures; m, meters. Sample types described in text and table 1. N/A, not applicable. XRD, X-ray diffraction. Analyses are presented in appendix 3. Onsite core recovery length is the original length measured in 2009. Cores are logged from bottom (0.0 ft) to the top of the sample relative to core lengths measured in 2013, which could be different than the onsite length (table 2). See appendix 2 for more detail on fossil and trace fossil observations.]

Drilling depth interval	Description from drilling speed and onsite observations	Descriptions of mud stream samples	Descriptions of core barrel samples
191–201 ft (58.2–61.3 m) Core run 14	Sand with clay layers at 193–198 ft and 201 ft	Bucket sample, 191–201 ft. Fine sand to silt with well-sorted, subangular to subrounded grains. Noncalcareous.	Core (3.2 ft onsite recovery). *2.7–3.1* Abrupt transition at 2.7 ft from clay below to medium-sorted, medium sand to silt with little clay above. Abundant dark grains. Calcareous. Similar to the sand from 0.0–1.3 ft but less well sorted. No bedding. *1.3–2.7* Greenish silty clay with very little silt, probably from 193–195 ft based on description and geophysical logs. Increases from calcareous at the bottom of the interval to very calcareous at the top. Shell at 2.3 ft. Sample collected for XRD analysis. *0.0–1.3* Very fine, olive-green sand to clay, with very little clay. Calcareous. Sand is well sorted with abundant dark grains. Clay content increases upward from 1.1–1.3 ft. No bedding. Sample collected for XRD analysis. Core catcher sample, possibly from 197 ft, based on logs. Fine sand to silt, with well-sorted, subangular to subrounded grains, including ash shards and magnetite. Noncalcareous. Bivalve fossil collected.
201–211 ft (61.3–64.3 m) Core run 15	Fine sand with clay at 201–202.5 ft and tighter clay at 205–207 ft	Bucket sample, 201–211 ft (minimal material recovered). Coarse sand to silt with subangular, subrounded to rounded grains. Noncalcareous. A few glass shards. Some or all of the material may have come from a different depth interval.	Core (1.7 ft onsite recovery). *0.2–1.7* Muddy silt with some fine sand. Well sorted, with not as many dark grains as below. Slightly calcareous. No bedding or laminations. Shell fragment. *0.0–0.2* Silt to clay with dark grains. Slightly calcareous. Abrupt transition from silty clay to muddy silt above. No bedding or laminations. Core catcher sample, probably from 207 ft, based on logs. Silt to clay with some small gypsum crystals. Calcareous.
211–221 ft (64.3–67.4 m) Core run 16	Sand with greenish sandy clay at 211–214 ft	Bucket sample, 211–221 ft. Coarse sand to silt with medium-sorted, subangular to rounded grains. Abundant dark grains. Calcareous.	Core (2.2 ft onsite recovery). *0.0–2.2* Sand to clay, with very little fine sand, mostly silt. Calcareous. Ostracod, clam, and unknown shell fragments from 1.4 to 2.1 ft. Some small magnetic black blotches from 2.0 to 2.2 ft. Core catcher sample, probably from 215 ft, based on logs. Fine sand to gray-green clay. Calcareous. Bivalve fragments. Fish bones(?) sampled.

Appendix 1. Descriptions of samples by type and drilling interval.—Continued

[Drilling depth interval, interval evaluated for sampling; those sampled for core are indicated by the core run number; depths listed in feet (ft), corresponding to drilling procedures; m, meters. Sample types described in text and table 1. N/A, not applicable. XRD, X-ray diffraction. Analyses are presented in appendix 3. Onsite core recovery length is the original length measured in 2009. Cores are logged from bottom (0.0 ft) to the top of the sample relative to core lengths measured in 2013, which could be different than the onsite length (table 2). See appendix 2 for more detail on fossil and trace fossil observations.]

Drilling depth interval	Description from drilling speed and onsite observations	Descriptions of mud stream samples	Descriptions of core barrel samples
221–231 ft (67.4–70.4 m) (No core sample)	Mostly sand, with perhaps a little sandy clay. Geophysical logs show increased resistivity and density values for the interval 224–232 ft, suggesting some lithification	Bucket sample, 221–231 ft. Coarse sand to silt with medium-sorted, subangular to rounded grains. A few small clumps of calcareous mud. Calcareous. Abundant ostracods; several were sampled.	N/A
231–241 ft (70.4–73.5 m) Core run 17	Sand with clay at 232.0–233.5 ft and 237–241 ft. Clay has a bluish tint	Bucket sample, 231–241 ft (minimal material recovered). Coarse to fine sand with medium- to well-sorted, subangular to rounded grains. Calcareous. Shell fragments. Some or all of the material may have come from a different depth interval.	Core, top 4.8 ft (7.3 ft total onsite recovery, divided). Top probably at 232 ft. *3.8–4.8* Clay with very little silt. Calcareous. Ostracods and unidentified, possible fossils. *3.6–3.8* Silty clay. Calcareous. Ostracods and unidentified, possible fossils. *0.0–3.6* Clay with very little silt. Calcareous. Possible bioturbation at 1.1 ft and indicated by centimeter-size ovals with rust-colored haloes at 0.8 ft. Otherwise, no visible laminations throughout the interval. Gastropods and other shells. Carbon residue, woody plant fragments, and tooth or bone fragments at 0.2 ft. Core, bottom 2.5 ft (7.3 ft total recovered, divided). *0.0–2.5* Silt to clay with massive clay from 0.0–0.3 ft. Calcareous. Possible bioturbation at 0.4 and 1.5 ft. Parallel lamina at 1.6 ft (faint) and at 2.0–2.5 ft. Vertebrate fragment at 1.7 ft, unidentified shell fragments at 0.4 to 0.8 ft. Sample taken at 1.2 ft for XRD analysis. Core catcher sample, probably from 241 ft. Tan-colored, fine silt to clay with some mica. Slightly calcareous.
241–251 ft (73.5–76.5 m) (No core sample)	Sand with clay at 243.0–244.0 ft and 249.5–251 ft	Bucket sample, 241–251 ft (little material recovered). Fine sand to silt with subangular to rounded grains. Noncalcareous. Magnetite grains. Shell fragments, glass bubble, ash shards.	N/A

Appendix 1. Descriptions of samples by type and drilling interval.—Continued

[Drilling depth interval, interval evaluated for sampling; those sampled for core are indicated by the core run number; depths listed in feet (ft), corresponding to drilling procedures; m, meters. Sample types described in text and table 1. N/A, not applicable. XRD, X-ray diffraction. Analyses are presented in appendix 3. Onsite core recovery length is the original length measured in 2009. Cores are logged from bottom (0.0 ft) to the top of the sample relative to core lengths measured in 2013, which could be different than the onsite length (table 2). See appendix 2 for more detail on fossil and trace fossil observations.]

Drilling depth interval	Description from drilling speed and onsite observations	Descriptions of mud stream samples	Descriptions of core barrel samples
251–261 ft (76.5–79.6 m) Core run 18	Sand 251–256 ft. Soft blue clay at 256–261 ft. Light-colored band 52–53 in. from top of core. Wide black bands between 35–39 in. from top of core.	Sieve sample, 251–261 ft. Fine sand to clay. Calcareous. Volume of the sieve sample is much greater than that of the bucket sample. Bucket sample, 251–261 ft (little material recovered). Medium sand to silt with subangular to rounded grains. Clay chunks. Slightly calcareous. Some or all of the material may have come from a different depth interval.	Core, top 4.8 ft (6.2 ft total onsite recovery, divided). *4.5–4.8* Silt to clay, grading upward from calcareous to more calcareous. At the bottom of this interval, a 0.1-ft-thick, olive-colored, silty clay layer is bounded above and below by two rust-colored laminations. Top of this core is probably at 256 ft depth. *3.9–4.5* Clay with faint, parallel laminations. Grades upward from noncalcareous to calcareous. *1.6–3.9* Clay with faint, parallel laminations. Noncalcareous. Possible burrow with rust-colored ring haloes at 1.8 ft. Possible burrows at 2.5 ft. Ostracods. *1.3–1.6* Clay with faint, parallel laminations. Calcareous. Ostracods. *0.5–1.3* Clay with faint, parallel laminations. Noncalcareous. Possible root trace at 0.7 ft. Possible burrow at 1.0 ft. Ostracods and other shells. *0.0–0.5* Clay with faint, parallel laminations. Calcareous. Core, bottom 1.4 ft (6.2 ft total recovered, divided). *0.0–1.4* Clay with faint parallel laminations. Calcareous. A couple of pebble-sized pieces of magnetite at 1.0 ft; samples collected. Ostracods and other possible fossils. Core catcher sample. Clay with faint laminations. Calcareous. Core piece, 0.7 ft long, recovered from subsequent run, probably from 261 ft. Fine sand to clay. Calcareous.

Appendix 1. Descriptions of samples by type and drilling interval.—Continued

[Drilling depth interval, interval evaluated for sampling; those sampled for core are indicated by the core run number; depths listed in feet (ft), corresponding to drilling procedures; m, meters. Sample types described in text and table 1. N/A, not applicable. XRD, X-ray diffraction. Analyses are presented in appendix 3. Onsite core recovery length is the original length measured in 2009. Cores are logged from bottom (0.0 ft) to the top of the sample relative to core lengths measured in 2013, which could be different than the onsite length (table 2). See appendix 2 for more detail on fossil and trace fossil observations.]

Drilling depth interval	Description from drilling speed and onsite observations	Descriptions of mud stream samples	Descriptions of core barrel samples
261–266 ft (79.6–81.1 m) Core run 19	Blue-gray clay	Bucket sample, 261–266 ft (minimal material recovered). Fine sand to silt with medium-sorted, subangular to rounded grains. Noncalcareous. A few ash shards. Some or all of the material may have come from a different depth interval.	Core (4.5 ft onsite recovery), top probably from 261 ft. *3.6–4.0* Gradual increase upward from clay to silt. Very calcareous. Parallel laminations. Ostracods in siltier interval. *1.6–3.6* Silt to clay, very little silt. Very calcareous. Parallel laminations. Slickenside measured 40º from parallel to core, opposite orientation to the one below. Ostracods and other shells. Diatoms at 2.8 ft. *0.0–1.6* Clay. Very calcareous. Parallel laminations. Slickenside measured 40º from parallel to core, opposite orientation to the one above. Ostracods. Core catcher sample. Fine sand to clay, mostly clay. Gypsum crystals. Calcareous. Abundant ostracods.
266–271 ft (81.1–82.6 m) Core run 20	Blue-gray clay.	Bucket sample, 266–271 ft (minimal material recovered). Fine sand to silt with medium-sorted, subangular to rounded grains, some or all of which may have come from a different depth interval. Slightly calcareous. Clumps of clay. Ostracods.	Core (3.8 ft onsite recovery). *3.1–3.5* Massive clay. Calcareous. Ostracods. *3.0–3.1* Silty clay. Calcareous. Ostracods. *1.7–3.0* Massive clay with 1-inch-thick ostracod bed at about 2.5 ft. Calcareous. *1.6–1.7* Silt to clay, mostly clay. Calcareous. Ostracods. *1.3–1.6* Clay. Calcareous. Ostracods. *1.0–1.3* Silt to clay, mostly clay. Calcareous. Ostracods. *0.5–1.0* Clay with ostracod coquina at about 0.9 ft. Faint laminations. Calcareous. *0.2–0.5* Silt to clay, mostly clay. Calcareous. *0.0–0.2* Clay with ostracods. Calcareous. Core catcher sample. Clay with very little silt. Calcareous. Ostracods.
271–276 ft (82.6–84.1 m) Core run 21	Blue-gray clay. Much of the core was deformed from drilling.	Bucket sample, 271–276 ft (minimal material recovered). Fine sand to clay with clay chunks. Calcareous. Some or all of the material may have come from a different depth interval.	Core (3.7 ft onsite recovery; core was deformed from drilling). *0.0–3.2* Massive blue clay with very little silt. Calcareous. Sample taken for XRD analysis at 1 ft. Difficult to tell, but appears to have no sedimentary structures or trace fossils. Ostracods are present throughout, especially abundant at about 1.4 ft. Core catcher sample, probably from 274–275 ft, based on logs. Clay with some dark fine sand grains. Abundant gypsum crystals, some mica. Calcareous. Ostracods.

Appendix 1. Descriptions of samples by type and drilling interval.—Continued

[Drilling depth interval, interval evaluated for sampling; those sampled for core are indicated by the core run number; depths listed in feet (ft), corresponding to drilling procedures; m, meters. Sample types described in text and table 1. N/A, not applicable. XRD, X-ray diffraction. Analyses are presented in appendix 3. Onsite core recovery length is the original length measured in 2009. Cores are logged from bottom (0.0 ft) to the top of the sample relative to core lengths measured in 2013, which could be different than the onsite length (table 2). See appendix 2 for more detail on fossil and trace fossil observations.]

Drilling depth interval	Description from drilling speed and onsite observations	Descriptions of mud stream samples	Descriptions of core barrel samples
276–291 ft (84.1–88.7 m) Core run 22	Mostly sand with some clay layers	Bucket sample, 276–281 ft. Fine sand to silt with medium-sorted, subangular to rounded grains. Very slightly calcareous. Bucket sample, 281–291 ft. Fine sand to silt with medium-sorted, subangular to rounded grains. Very slightly calcareous. Some clay balls, ostracods, and a few ash shards.	Viscous fluid sample, scooped. Fine sand to silt with medium-sorted, subangular to rounded grains. Noncalcareous. Core (0.9 ft onsite recovery, probably from about 280 ft, based on logs). *0.0–0.8* Silty, blue clay. Fine, wavy to parallel laminations in upper 0.6 ft; lower 0.3 ft very massive. Calcareous throughout. Ostracods. Core was coated in sand. Sample collected at 0.2 ft for XRD analysis. Core catcher sample. Clay with some fine sand. Mica, ostracods. Calcareous.
291–301 ft (88.7–91.7 m) Core run 23	Sand with gray clay below 295 ft	Bucket sample, 291–301 ft. Fine sand to silt with subangular to rounded grains. Very slightly calcareous	Core piece, 0.4 ft long, from top of core, probably from 295 ft. Greenish-gray clay with some fine sand interbeds. Dark patches. Disrupted interbeds with rip-up clasts(?). Breccia from a slump or debris flow. Calcareous. Shell fragments. Core (4.9 ft onsite recovery, probably from 295–300 ft). *4.0–5.0* Abrupt change in color above 4.0 ft to dark gray, silty clay with a thin layer of lighter color clay at 4.3 ft. Grades to clay in the top 0.3 ft of the interval. Very bioturbated below 4.2 ft, with parallel laminations from 4.4 to 4.8 ft and wavy laminations above that. Ostracods and abundant shell fragments. Calcareous throughout. *0.0–4.0* Tan clay with very little silt. Very bioturbated except for a 0.1-ft- thick zone of faint laminations at 1 ft. Burrows, gastropods, and other shell fragments within the interval. Root traces at 2.7 ft. Calcareous throughout. Abrupt change in color above 4.0 ft. Core catcher sample. Massive gray clay, calcareous. Sample collected for XRD analysis

Appendix 1. Descriptions of samples by type and drilling interval.—Continued

[Drilling depth interval, interval evaluated for sampling; those sampled for core are indicated by the core run number; depths listed in feet (ft), corresponding to drilling procedures; m, meters. Sample types described in text and table 1. N/A, not applicable. XRD, X-ray diffraction. Analyses are presented in appendix 3. Onsite core recovery length is the original length measured in 2009. Cores are logged from bottom (0.0 ft) to the top of the sample relative to core lengths measured in 2013, which could be different than the onsite length (table 2). See appendix 2 for more detail on fossil and trace fossil observations.]

Drilling depth interval	Description from drilling speed and onsite observations	Descriptions of mud stream samples	Descriptions of core barrel samples
301–306 ft (91.7–93.3 m) Core run 24	Gray clay	Bucket sample, 301–306 ft (minimal material recovered). Fine sand to silt with subangular to rounded grains, some or all of which may have come from a different depth interval. Mud clumps	Core (5 ft onsite recovery). *0.0–5.0* Massive gray clay with very little silt and some mica. Faint laminations at the bottom 2 ft or so, with faint light and dark laminations, root trace, and other evidence of bioturbation at the bottom 0.1 ft. Ostracod at 2.4 ft; possible bone fragments at 2.9 ft. Otherwise, almost no sedimentary structures, shells, burrows, and so forth; possibly completely bioturbated. Noncalcareous from 0–4.2 ft; calcareous above that. Sample taken from 1.7 ft for XRD analysis. Sample taken from 0.2 ft was examined for diatoms but none were found. Deformation caused by drilling from 3.8–4.2 ft.
306–311 ft (93.3–94.8 m) Core run 25	Consolidated gray clay. Field photos show angular laminations and dark gray or greenish, oval or round spots of about 1-2 inches in diameter in the top 1 foot of the core recovered.	Bucket sample, 306–311 ft (minimal material recovered). Fine sand to silt with subangular to rounded grains, some or all of which may have come from a different depth interval. Mud clumps	Core (2 ft onsite recovery). *0.0–1.9* Gray clay with some silt and some mica. No bioturbation or shells. Massive for the bottom 0.2 ft; abrupt transition to parallel laminations above 0.2 ft. Noncalcareous throughout. Core catcher sample. Silt to clay, very calcareous. Faintly laminated.
311–316 ft (94.8–96.3 m) Core run 26	Sandy clay or a few stringers of sand within mostly gray clay. A 1.5-inch light-tan band occurs about 3.5 ft from bottom of core.	Bucket sample, 311–316 ft (minimal material recovered). Fine sand to silt with subangular to rounded grains, some or all of which may have come from a different depth interval. Mud clumps	Core piece, 0.2 ft from top of core. Clay with some fine sand grains. Noncalcareous. Core (4.8 ft onsite recovery). *0.0–4.5* Gray clay with some silt and some mica. No bioturbation or shells, but may contain organic remains. Parallel laminations throughout. Noncalcareous throughout. A 1.5-inch light-rust-colored, laminated band occurs at about 3.2 ft and exhibits less shrinkage than the rest of the core. XRD analyses of samples from the band at 3.2 ft and above the band at 3.8 ft show high magnesium calcite in the band and low magnesium calcite outside of the band.

Appendix 1. Descriptions of samples by type and drilling interval.—Continued

[Drilling depth interval, interval evaluated for sampling; those sampled for core are indicated by the core run number; depths listed in feet (ft), corresponding to drilling procedures; m, meters. Sample types described in text and table 1. N/A, not applicable. XRD, X-ray diffraction. Analyses are presented in appendix 3. Onsite core recovery length is the original length measured in 2009. Cores are logged from bottom (0.0 ft) to the top of the sample relative to core lengths measured in 2013, which could be different than the onsite length (table 2). See appendix 2 for more detail on fossil and trace fossil observations.]

Drilling depth interval	Description from drilling speed and onsite observations	Descriptions of mud stream samples	Descriptions of core barrel samples
316–321 ft (96.3–97.8 m) Core run 27	Gray clay with a coarser grained layer about 1.5 ft from the top of the core.	Bucket sample, 316–321 ft (minimal material recovered). Fine sand to silt with subangular to rounded grains, some or all of which may have come from a different depth interval. Mud clumps	Core (5 ft onsite recovery). *0.0–4.5* Gray clay with very little silt and some mica. Noncalcareous throughout. Parallel laminations throughout. The bottom 2.8 ft consists of many light-colored laminations about 2 millimeters thick; no pattern is observed. A few ostracods and other shells observed within 2.5–4.4 ft. A thin bed of bivalves and possible gastropods at 3.1 ft is surrounded by light-rust-colored sediment. Possible light-rust-colored oval burrow at 4.4 ft. Sample taken from 0.7 ft was examined for diatoms but none were found. Core piece, 0.1 ft from bottom of core. Clay with some fine sand grains. Noncalcareous.
321–326 ft (97.8–99.4 m) Core run 28	Gray clay. The top 2.7 ft of the core was deformed from drilling	Bucket sample, 321–326 ft (minimal material recovered). Fine sand to silt with subangular to rounded grains, some or all of which may have come from a different depth interval. Ostracods and gastropod fragments	Core (4.6 ft onsite recovery). *0.0–4.3* Gray clay with some silt and less mica than above. Slightly calcareous. No sand interbeds. No laminations visible, but difficult to tell because the core was deformed by drilling from 1.6 to 4.3 ft. A light-rust-colored bed at 2.5 ft is very calcareous. Sample taken for XRD analysis at 2.7 ft. Core catcher sample. Silt to clay with light and dark laminations. Noncalcareous.

Appendix 2. Depth intervals where fossils or other evidence of life were observed.

[Observations and identifications were made in 2012 by M.E. Benson and J.K. Davis, in 2013 by G. Skipp, and in 2014 by M.E. Benson. Refer to appendix 1 for detailed descriptions of samples and figure 7 for positions of core samples within the well. Measurements in inches (in); centimeters (cm); millimeters (mm); feet (ft); meters (m). N/A, not applicable]

Drilling depth interval	Sample type	Year of observation*	Measured length of core sample*	Distance measured from bottom of core sample*	Observation(s)	Comments
70–80 ft (21.3–24.4 m) Core run 2	Core catcher	2014	N/A	N/A	Diatoms	One small sample of gray silty clay was examined by M.E. Benson and found to contain a low-diversity diatom assemblage consisting of centric diatoms of the tentatively identified centric diatom species *Aulacoseira distans*, and *Stephanodiscus* sp., as well as possibly other genera in the Stephanodiscaceae family.
131–141 ft (39.9–43.0 m) Core run 11	Core	2013	10.0 in (25.4 cm)	8–10 in (20–25 cm)	Possible bioturbation	
171–191 ft (52.1–58.2 m) Core run 13	Core	2012	47.2 in (120.0 cm)	20–24 in (50–60 cm)	Ostracods	A few ostracods observed.
181–191 ft (55.2–58.2 m)	Bucket sample	2013	N/A	N/A	Clam shells	Very tiny shells collected.
191–201 ft (58.2–61.3 m) Core run 14	Core	2013	37.0 in (94.0 cm)	28 in (71 cm)	Shell	Single unidentified shell observed.
	Core catcher	2013	N/A	N/A	Bivalve shell	Tiny shell collected.
201–211 ft (61.3–64.3 m) Core run 15	Core	2013	20.0 in (50.8 cm)	12 in (30 cm)	Shell fragment	Single unidentified shell fragment observed.
211–221 ft (64.3–67.4 m) Core run 16	Core	2012	24.8 in (63.0 cm)	17–25 in (43–63 cm)	Ostracods, clam, shell fragments	Whole ostracod and unidentified shell fragments collected 19 in (48 cm) above the bottom of the core.
		2013	26.0 in (66.0 cm)	23 in (58 cm)	Shell fragments	Unidentified shell fragments observed.
	Core catcher	2013	N/A	N/A	Bivalve fragments, fish bones?	Bones (possible fish bones) collected.
221–231 ft (67.4–70.4 m)	Bucket sample	2013	N/A	N/A	Ostracods	Abundant ostracods; several collected.

*Measured lengths of core samples and distances relative to their bottoms are listed by year because measurements varied by year of observation (see table 2).

Appendix 2. Depth intervals where fossils or other evidence of life were observed.—Continued

[Observations and identifications were made in 2012 by M.E. Benson and J.K. Davis, in 2013 by G. Skipp, and in 2014 by M.E. Benson. Refer to appendix 1 for detailed descriptions of samples and figure 7 for positions of core samples within the well. Measurements in inches (in); centimeters (cm); millimeters (mm); feet (ft); meters (m). N/A, not applicable]

Drilling depth interval	Sample type	Year of observation*	Measured length of core sample*	Distance measured from bottom of core sample*	Observation(s)	Comments
231–241 ft (70.4–73.5 m) Core run 17	Core (top piece)	2012	55.9 in (142.0 cm)	52 in (132 cm)	Ostracods	
				46 in (118 cm)	Fossil	Unidentified fossil collected.
				36–56 in (92–142 cm)	Ostracod, unknown white circular grains	Unknown fine white circular grains may or may not be fossils.
				34 in (86 cm)	Possible gastropod	Possible gastropod collected.
				33–35 in (84–89 cm)	Shell fragments	Unidentified shell fragments collected.
				32–36 in (82–92 cm)	Gastropods	A few gastropods were observed.
				13 in (32 cm)	Gastropods, bioturbation	
				9 in (24 cm)	Burrow	Burrow sampled.
				5 in (12 cm)	Possible black shells	Black-colored specimens that may be shells were collected.
				4–13 in (9–32 cm)	Gastropod, unknown white circular grains	Unknown fine white circular grains may or may not be fossils.
				2 in (4 cm)	Carbon residue, woody plant fragments, tooth or bone fragments	
		2013	57.5 in (146.1 cm)	10 in (25 cm)	Possible bioturbation	Possible bioturbation indicated by 1-cm-size ovals with rust-colored haloes.

*Measured lengths of core samples and distances relative to their bottoms are listed by year because measurements varied by year of observation (see table 2).

Appendix 2. Depth intervals where fossils or other evidence of life were observed.—Continued

[Observations and identifications were made in 2012 by M.E. Benson and J.K. Davis, in 2013 by G. Skipp, and in 2014 by M.E. Benson. Refer to appendix 1 for detailed descriptions of samples and figure 7 for positions of core samples within the well. Measurements in inches (in); centimeters (cm); millimeters (mm); feet (ft); meters (m). N/A, not applicable]

Drilling depth interval	Sample type	Year of observation*	Measured length of core sample*	Distance measured from bottom of core sample*	Observation(s)	Comments
231–241 ft (70.4–73.5 m) Core run 17	Core (bottom piece)	2012	28.3 in (72.0 cm)	20 in (50 cm)	Vertebrate fossil	Fragments of vertebrate remains collected.
				7 in (18 cm)	Shell fragments	Unidentified shell fragments collected.
				5–9 in (12–22 cm)	Shell fragments	Unidentified shell fragments.
		2013	29.4 in (74.7 cm)	18 in (46 cm)	Possible bioturbation	
				5 in (12 cm)	Possible bioturbation	
241–251 ft (73.5–76.5 m)	Bucket sample	2013	N/A	N/A	Shell fragments	Unidentified shell fragments observed.
251–261 ft (76.5–79.6 m) Core run 18	Core (top piece)	2012	51.6 in (131.0 cm)	33 in (83 cm)	Ostracods	
				13 in (32–34 cm)	Shell fragments	Unidentified shell fragments were collected.
				0–20 in (1–51 cm)	Ostracods	Ostracods were observed throughout this interval.
		2013	57.5 in (146.1 cm)	30 in (76 cm)	Burrows	Possible burrows.
				22 in (55 cm)	Burrow	Possible burrow indicated by rust-colored haloes.
				12 in (30 cm)	Burrow	Possible burrow.
				8 in (20 cm)	Root trace	Possible root trace.
	Core (bottom piece)	2012	13.8 in (35.0 cm)	0–14 in (0–35 cm)	Ostracods, unknown circular white grains, shell fragments	Ostracods and unknown fine white circular grains, which may or may not be fossils, were observed throughout the core piece. Unidentified shell fragments were collected 3 in (7 cm) above the bottom of the core piece.

*Measured lengths of core samples and distances relative to their bottoms are listed by year because measurements varied by year of observation (see table 2).

Appendix 2. Depth intervals where fossils or other evidence of life were observed.—Continued

[Observations and identifications were made in 2012 by M.E. Benson and J.K. Davis, in 2013 by G. Skipp, and in 2014 by M.E. Benson. Refer to appendix 1 for detailed descriptions of samples and figure 7 for positions of core samples within the well. Measurements in inches (in); centimeters (cm); millimeters (mm); feet (ft); meters (m). N/A, not applicable]

Drilling depth interval	Sample type	Year of observation*	Measured length of core sample*	Distance measured from bottom of core sample*	Observation(s)	Comments
261–266 ft (79.6–81.1 m) Core run 19	Core	2012	45.7 in (116.0 cm)	0–46 in (0–116 cm)	Ostracods	Ostracods abundant throughout this core sample, especially at 4 in (10 cm) above the bottom of the sample. Samples collected at 17 in (43 cm) and 36 in (91 cm) above the bottom of the sample.
				34 in (86 cm)	Diatoms, ostracods	A few diatoms were present in a sample containing ostracods. M.E. Benson observed a low-diversity diatom assemblage dominated by the tentatively identified small centric species *Aulacoseira distans* and the large pennate species *Anomoeoneis sphaerophora f. costata*. Additional pennate genera, possibly of the Achnanthidiaceae and Fragilariaceae families, as well as one specimen resembling the genus *Surirella*, were also observed.
				22–30 in (56–76 cm)	Shell fragments	Unknown shell fragments.
		2013	48.0 in (121.9 cm)	44–46 in (112–116 cm)	Ostracods	Abundant ostracods observed within a silty interval.
	Core catcher	2013	N/A	N/A	Ostracods	Abundant ostracods throughout the sample.
266–271 ft (81.1–82.6 m) Core run 20	Core	2012	39.4 in (100.0 cm)	0–39 in (0–100 cm)	Ostracods	Ostracods abundant throughout the sample, with ostracod coquinas at 10–11 in (25–28 cm), 25–26 in (64–65 cm), and 30 in (75 cm) above the bottom. Shell fragments and ostracods collected from the lower two coquinas.
				35 in (90 cm)	Unknown specimen	An unidentified specimen of brown color was collected.
		2013	42.0 in (106.7 cm)	30 in (76 cm)	Ostracods	Ostracod coquina about 1 in (3 cm) thick.
				12 in (30 cm)	Ostracods	
				2 in (6 cm)	Ostracods	
	Core catcher	2013	N/A	N/A	Ostracods	
	Bucket sample	2013	N/A	N/A	Ostracods	

*Measured lengths of core samples and distances relative to their bottoms are listed by year because measurements varied by year of observation (see table 2).

Appendix 2. Depth intervals where fossils or other evidence of life were observed.—Continued

[Observations and identifications were made in 2012 by M.E. Benson and J.K. Davis, in 2013 by G. Skipp, and in 2014 by M.E. Benson. Refer to appendix 1 for detailed descriptions of samples and figure 7 for positions of core samples within the well. Measurements in inches (in); centimeters (cm); millimeters (mm); feet (ft); meters (m). N/A, not applicable]

Drilling depth interval	Sample type	Year of observation*	Measured length of core sample*	Distance measured from bottom of core sample*	Observation(s)	Comments
271–276 ft (82.6–84.1 m) Core run 21	Core	2012	35.4 in (90.0 cm)	0–35 in (0–90 cm)	Ostracods	Ostracods observed throughout the core sample. They are abundant 16–17 in (41–42 cm) above the base of the sample. Specimens collected from 17 in (42 cm) and 1 in (3 cm) above the bottom of the core sample.
	Core catcher	2013	N/A	N/A	Ostracods	
276–291 ft (84.1–88.7 m) Core run 22	Core	2012	9.1 in (23.0 cm)	0–9 in (0–23 cm)	Ostracods	Ostracods observed throughout the whole sample. Specimens collected 7 in (17 cm) above the bottom of the core sample.
	Core catcher	2013	N/A	N/A	Ostracods	
291–301 ft (88.7–91.7 m) Core run 23	Core piece at top	2013	N/A	N/A	Shell fragments	Unidentified shell fragments observed.
	Core	2012	57.9 in (147.0 cm)	50–58 in (127–147 cm)	Ostracods, shell fragments	Ostracods and unknown 5-mm-size shell fragments observed. J.K. Davis collected samples of ostracods and other fossils from 53 in (135 cm) and 54–55 in (137–140 cm).
				42–46 in (107–117 cm)	Gastropods, shell fragments	Gastropods and unknown 5-mm-size shell fragments observed.
				30–42 in (77–107 cm)	Shell fragments	A few unknown, 2-mm-size shell fragments observed.
				32 in (81 cm)	Bioturbation, root traces, gastropods	Bioturbation, possible root traces, and fragments of gastropods observed.
				19–26 in (47–67 cm)	Shell fragments	Unknown 1-mm-size shell fragments observed.
		2013	60.0 in (152.4 cm)	0–50 in (0–128 cm)	Bioturbation, burrows, shell fragments	Sample shows intense bioturbation, with burrows at 18 in (46 cm), 19 in (49 cm), 24 in (61 cm), 30 in (76 cm), and possibly at 2 in (6 cm) above bottom of the core, respectively. Shell fragments were also observed at 24 in (61 cm).
				48–58 in (122–147 cm)	Shell fragments	Abundant shell fragments.
				17 in (43 cm)	Gastropod	A small gastropod observed.

*Measured lengths of core samples and distances relative to their bottoms are listed by year because measurements varied by year of observation (see table 2).

Appendix 2. Depth intervals where fossils or other evidence of life were observed.—Continued

[Observations and identifications were made in 2012 by M.E. Benson and J.K. Davis, in 2013 by G. Skipp, and in 2014 by M.E. Benson. Refer to appendix 1 for detailed descriptions of samples and figure 7 for positions of core samples within the well. Measurements in inches (in); centimeters (cm); millimeters (mm); feet (ft); meters (m). N/A, not applicable]

Drilling depth interval	Sample type	Year of observation*	Measured length of core sample*	Distance measured from bottom of core sample*	Observation(s)	Comments
301–306 ft (91.7–93.3 m) Core run 24	Core	2012	56.3 in (143.0 cm)	2 in (5 cm)	Bioturbation, root traces	Root traces and other bioturbation features were observed. M.E. Benson examined the sample for diatoms and found none.
		2013	60.0 in (152.4 cm)	35 in (85 cm)	Possible bone fragments	
				29 in (73 cm)	Ostracod	
316–321 ft (96.3–97.8 m) Core run 27	Core	2012	53.1 in (135.0 cm)	49–53 in (125–135 cm)	Shell fragments	A few, unidentified 1-mm-size shell fragments observed.
				37–49 in (95–125 cm)	Ostracods	A few ostracods observed.
				37 in (95 cm)	Gastropods, bivalves	Horizon of abundant gastropods and bivalves (possible clams). Samples collected.
				30–37 in (75–95 cm)	Ostracods	A few ostracods observed.
				8 in (21 cm)		M.E. Benson examined a sample for diatoms within a white-colored band but found none.
		2013	54.0 in (137.2 cm)	53 in (137 cm)	Burrow	Possible burrow indicated by a rust-colored oval.
				37 in (95 cm)	Bivalves, burrow	Horizon of abundant bivalves. Possible burrow surrounded by light rust-colored sediment.
321–326 ft (97.8–99.4 m)	Bucket sample	2013	N/A	N/A	Ostracods and gastropods	Ostracods and gastropod fragments were observed in this sample, but may have come from a higher interval within the well.

*Measured lengths of core samples and distances relative to their bottoms are listed by year because measurements varied by year of observation (see table 2).

Appendix 3. Results of analysis by X-ray powder diffraction

[Depth in feet (ft); meters (m); in., inch. Refer to appendix 1 for detailed descriptions of samples. Minerals are listed in order of peak X-ray intensity]

Drilling interval	Sample type	Description of specimen collected	Bulk X-ray minerology
30–40 ft (9.1–12.2 m)	Hopper, fine fraction	Fine sand	Quartz, anorthite, albite, cristobalite, potassium feldspar, amphibole, mica.
70–80 ft (21.3–24.4 m)	Core catcher	Clay from about 77 ft depth	Quartz, plagioclase feldspar, calcite, cristobalite, clay, mica.
70–80 ft (21.3–24.4 m)	Core catcher	Silt from about 77 ft depth	Quartz, plagioclase feldspar, cristobalite, calcite, clay, mica.
80–90 ft (24.4–27.4 m)	Core catcher	Very fine sand to clay, possibly from about 85 ft depth	Quartz, albite, cristobalite, potassium feldspar, mica, smectite.
119–125 ft (36.3–38.1 m)	Core catcher	Fine sand to silt, probably from somewhere between 121 and 125 ft depth	Quartz, plagioclase feldspar, cristobalite, potassium feldspar, clay, pyrite?
191–201 ft (58.2–61.3 m)	Core	Silty clay taken from approximately 2 ft above the bottom of the core	Quartz, plagioclase feldspar, cristobalite, potassium feldspar, clay.
191–201 ft (58.2–61.3 m)	Core	Very fine sand taken from the lower foot of the core	Cristobalite, quartz, plagioclase feldspar, mica.
231–241 ft (70.4–73.5 m)	Core	Clay taken from 14 in. above the bottom of the bottom core piece, probably at about 239–240 ft depth	Quartz, plagioclase feldspar, cristobalite, calcite, clay, mica, kaolinite.
271–276 ft (82.6–84.1 m)	Core	Clay taken from 11 in. above the bottom of the core, at about 273 ft depth	Quartz, calcite, plagioclase feldspar, cristobalite, potassium feldspar, clay, mica.
276–291 ft (84.1–88.7 m)	Core	Clay taken from 2 in. above the bottom of the core, probably at about 280 ft depth	Quartz, calcite, plagioclase feldspar, cristobalite, clay, potassium feldspar, mica, kaolinite.
291–301 ft (88.7–91.7 m)	Core catcher	Clay from about 300 ft depth	Quartz, calcite, plagioclase feldspar, cristobalite, clay, potassium feldspar, mica, kaolinite.
301–306 ft (91.7–93.3 m)	Core	Clay taken from 20 in. above the bottom of the core, at about 304 ft depth	Plagioclase feldspar, quartz, cristobalite, dolomite, potassium feldspar, clay, mica, kaolinite.
311–316 ft (94.8–96.3 m)	Core	Clay taken at 45 in. from the bottom of the core, sampled above a light-rust-colored band at 38 in. Sample probably from a depth of about 312 ft	Cristobalite, plagioclase feldspar, quartz, potassium feldspar, calcite, clay, kaolinite, mica.
311–316 ft (94.8–96.3 m)	Core	Sample taken from a light-rust-colored, laminated band 38 in. above the bottom of the core, probably at about 313 ft depth	High-magnesium calcite, plagioclase feldspar, cristobalite, quartz, potassium feldspar, clay, mica.
321–326 ft (97.8–99.4 m)	Core	Clay taken from 32 in. above the bottom of the core, at about 322 ft depth	Quartz, plagioclase feldspar, cristobalite, potassium feldspar, clay, calcite, kaolinite, mica.

Publishing support provided by the U.S. Geological Survey Science
Publishing Network, Rolla Publishing Service Center and
Denver Publishing Service Center

For more information concerning the research in this report, contact the
Director, Crustal Geophysics and Geochemistry Science Center
U.S. Geological Survey
Box 25046, Mail Stop 964
Denver, CO 80225
http://crustal.usgs.gov/

ISSN 2327-638X (online)
http://dx.doi.org/10.3133/ds918